

CLEAVAGE OF DUPLEX DNA USING TWO-PHOTON EXCITATION OF  
N-(ALKOXY)PYRIDINE THIONES

By

Michael Ruzic-Gauthier

Submitted in partial fulfillment of the requirements  
for the degree of Master of Science

at

Dalhousie University  
Halifax, Nova Scotia  
July 2013

© Copyright by Michael Ruzic-Gauthier, 2013

## DEDICATION

For my Family  
&  
Girlfriend Ali  
Love you guys always

## TABLE OF CONTENTS

<b>LIST OF TABLES</b> .....	<b>v</b>
<b>LIST OF FIGURES</b> .....	<b>vi</b>
<b>ABSTRACT</b> .....	<b>x</b>
<b>LIST OF ABBREVIATIONS USED</b> .....	<b>xi</b>
<b>ACKNOWLEDGEMENTS</b> .....	<b>xiii</b>
<b>Chapter 1 Introduction</b> .....	<b>1</b>
<b>1. Two-Photon Absorption</b> .....	<b>1</b>
1.1 Two-photon Absorption: Introduction .....	1
1.1.1 Two-photon Absorption: Optic Fundamentals .....	2
1.1.2 Two-Photon Absorption: Applications .....	5
1.1.3 Two-photon Absorption: Cross Section .....	9
1.1.3.1 Two-photon Absorption: Cross Sections- Measurements .....	10
1.1.3.1.1 Two-photon Excited Fluorescence (TPEF) .....	11
1.1.4 Two-Photon Absorption: Laser as a Light Source .....	13
<b>Chapter 2 Radicals in Biological Systems</b> .....	<b>14</b>
<b>2. Free Radicals: Oxidation of Biological Molecules</b> .....	<b>14</b>
2.1 Free Radicals: Formation .....	14
2.1.1 Free Radicals: Oxidative Damage to DNA .....	15
2.1.1.1 Free Radicals: Mechanisms of Oxidative DNA Damage .....	16
2.1.2 Free Radicals: DNA Photocleaving Reagents .....	20
2.1.2.1 Free Radicals: Photoradical Generators N-alkoxypyridinethiones .....	22
2.1.3 Free Radicals: Applications Photodynamic Therapy .....	26
2.1.3.1 Free Radicals: Applications- Two-photon Excitation PDT (2PE-PDT) .....	28
2.1.4 Free Radicals: Observing DNA Damage via Gel Electrophoresis .....	29
2.2 Scope of this Thesis .....	31
<b>Chapter 3 Results and Discussion</b> .....	<b>33</b>
3.1 Observing and Quantifying DNA Strand Breaks .....	34
3.2 Experiments with pBR 322 DNA and N-Hydroxypyridinethione <b>1a</b> .....	35

3.3 Experiments with pBR 322 DNA and N-Benzoyloxypyridinethione <b>1b</b> .....	39
3.4 Experiments with pBR322 DNA and N-Naphthoyloxypyridinethione <b>1c</b> .....	41
3.5 Experiments with pBR 322 DNA and N-Acetoxylopyridinethione <b>1d</b> .....	43
3.6 Comparisons Between O-acyl Radical Generators <b>1b - d</b> .....	45
3.7 Experiments with pBR 322 DNA and N-Benzoyloxypyridinethione <b>1e</b> .....	49
3.8 Experiments with pBR 322 DNA and N-t-Butoxylopyridinethione <b>1f</b> .....	53
3.9 Comparisons between Radical Generators <b>1a - 1f</b> .....	55
3.10 Time Dependent Efficiency Experiment with pBR 322 DNA and N-Hydroxylopyridinethione <b>1a</b> .....	58
<b>Chapter 4 Two-photon decomposition of N-anthracenoyloxypyridinethione.....</b>	<b>62</b>
<b>4.1 Introduction</b> .....	<b>62</b>
<b>4.2 Results and Discussion.</b> .....	<b>64</b>
4.2.1 Two-photon Cross Section: Mathematical Equations.....	64
4.2.2 Two-photon Cross Section: Experimental Results.....	66
<b>Chapter 5 experimental.....</b>	<b>71</b>
5.1 General Methods .....	71
5.2 Synthesis of Compounds <b>1b - 1g</b> .....	72
5.3 Materials and Methods of DNA Studies .....	76
5.3.1 Laser Irradiation Experiments: Modification of pBR 322 DNA.....	77
5.3.2 Determination of Strand Breaks by Gel Electrophoresis .....	77
5.4 Procedure for Measuring Two-photon Cross Section .....	78
<b>Chapter 6 Conclusions and Future Work .....</b>	<b>79</b>
6.1 Conclusions and Future Work: DNA Strand Cleavage Study .....	79
6.2 Conclusions and Future Work: Photodecomposition Study .....	80
<b>References.....</b>	<b>82</b>
<b>Appendix Copyright Permission .....</b>	<b>91</b>

## LIST OF TABLES

Table 1. Comparison of the two-photon cross sections for the decomposition of compounds <b>1b</b> - <b>d</b> , and their ability to cause DNA strand cleavage upon irradiation at 775 nm. ....	46
Table 2. Average conversion percentages to open-circular conformation upon irradiation at 775 nm for 3h. ....	56
Table 3. Effect of structure on the two-photon cross section for the photodecomposition of <i>N</i> -alkoxy pyridinethiones (Schepp, unpublished results). <sup>[77]</sup> .....	62

## LIST OF FIGURES

Figure 1. Energy diagram depicting one- and two-photon absorption.....	3
Figure 2. Fluorescence from a concentrated solution of a fluorophore using (TOP) two-photon excitation and (BOTTOM) one-photon excitation. Taken from ref. 22 ( <i>use of picture granted by copyright holder</i> ) .....	6
Figure 3. Fluorescence from a dilute solution of a fluorophore using (TOP beam) two-photon excitation and (BOTTOM beam) one-photon excitation. Taken from ref. 22 ( <i>use of picture granted by copyright holder</i> ) .....	8
Figure 4. Structures of chromophores <sup>[25]</sup> that exemplify general structural features for 2PA enhancements. ....	10
Figure 5. Schematic of the setup for a two-photon induced fluorescence experiment.....	12
Figure 6. Homolytic bond cleavage resulting in radical formation.....	14
Figure 7. Structure of a nucleotide, with the nucleobase and 2'-deoxyribose sugar moieties highlighted. It should be noted that an adenine base is used in this structure but any of the other three nucleobases can appear in this position linked with a nitrogen-carbon bond. ....	16
Figure 8. DNA bases with ring positions numbered. ....	17
Figure 9. Products of ·OH radical addition (OH-adducts) and abstraction (N-centered radical) from a guanine base.....	18
Figure 10. 2'-Deoxyribose sugar with labeled positions.....	19
Figure 11. General structure of <i>N</i> -alkoxypyridinethiones. ....	22
Figure 12. Structure of <i>N</i> -hydroxypyridinethione.....	22
Figure 13. General structure of Barton esters, where R represents an alkyl group. ....	23
Figure 14. Illustration of the basic process of PDT.....	27
Figure 15. Hypothetical result for the separation of supercoiled and open-circular DNA after migration through an agarose matrix, and a UV illuminated picture of the gel has been acquired. $X_v$ and $X_t$ represent voltage of the applied electric field ( $v$ ) and the time ( $t$ ), which the electric field has been applied for. Darkened strips represent the fluorescent bands indicating the presence of DNA. ....	31
Figure 16. Structures <i>N</i> -oxypyridinethiones <b>1a</b> - <b>1f</b> .....	32

Figure 17. Gel electrophoresis analysis of pBR 322 DNA (0.5  $\mu\text{g}/\mu\text{L}$  in 10 mM Tris-HCl 1.0 mM EDTA buffer, pH 8.0): (lane 2) upon irradiation of *N*-hydroxypyridinethione **1a** (4.45 mM in acetonitrile) for 3 h by a femtosecond laser at 775 nm and (lane 1) upon irradiation for 3 h by a femtosecond laser at 775 nm in the absence of **1a**. ..... 35

Figure 18. Gel electrophoresis analysis of pBR 322 DNA (0.5  $\mu\text{g}/\mu\text{L}$  in 10 mM Tris-HCl 1.0 mM EDTA buffer, pH 8.0): (lane 3) upon irradiation of *N*-hydroxypyridinethione **1a** (4.45 mM in acetonitrile) for 3 h by a femtosecond laser at 775 nm; (lane 2) with **1a** (4.45 mM in acetonitrile) in the dark for 3 h, and (lane 3) upon irradiation for 3 h by a femtosecond laser at 775 nm in the absence of **1a**. ..... 37

Figure 19. Gel electrophoresis analysis of pBR 322 DNA (0.5  $\mu\text{g}/\mu\text{L}$  in 10 mM Tris-HCl 1.0 mM EDTA buffer, pH 8.0): (lane 2) upon irradiation of **1b** (4.45 mM in acetonitrile) for 3 h by a femtosecond laser at 775 nm and (lane 1) upon irradiation for 3 h by a femtosecond laser at 775 nm in the absence of **1b**. ..... 40

Figure 20. Gel electrophoresis analysis of pBR 322 DNA (0.5  $\mu\text{g}/\mu\text{L}$  in 10 mM Tris-HCl 1.0 mM EDTA buffer, pH 8.0): (lane 3) upon irradiation of *N*-naphthoxyloxy pyridinethione **1c** (4.45 mM in acetonitrile) for 3 h by a femtosecond laser at 775 nm; (lane 2) upon irradiation of **1a** by a femtosecond laser at 775 nm for 3 h; and (lane 1) upon irradiation by a femtosecond laser at 775 nm for 3 h in the absence of any additive compound. .... 42

Figure 21. Gel electrophoresis analysis of pBR 322 DNA (0.5  $\mu\text{g}/\mu\text{L}$  in 10 mM Tris-HCl 1.0 mM EDTA buffer, pH 8.0): (lane 2) upon irradiation of *N*-acetoxy pyridinethione **1d** (4.45 mM in acetonitrile) for 3 h by a femtosecond laser at 775 nm and (lane 1) upon irradiation by a femtosecond laser at 775 nm for 3 h in the absence of **1d**. ..... 44

Figure 22. Formation and decarboxylation of carboxyl radicals. Rate constants<sup>[142]</sup> are for decarboxylation in acetonitrile. Ar = aryl or naphthyl group; R = alkyl group. .... 47

Figure 23. Gel electrophoresis analysis of pBR 322 DNA (0.5  $\mu\text{g}/\mu\text{L}$  in 10 mM Tris-HCl 1.0 mM EDTA buffer, pH 8.0): (lane 2) upon irradiation of *N*-benzyloxy pyridinethione **1e** (4.45 mM in acetonitrile) for 3 h by a femtosecond laser at 775 nm and (lane 1) upon irradiation by a femtosecond laser at 775 nm for 3 h in the absence of **1e**. ..... 49

Figure 24. Gel electrophoresis analysis of pBR 322 DNA (0.5  $\mu\text{g}/\mu\text{L}$  in 10 mM Tris-HCl 1.0 mM EDTA buffer, pH 8.0): (lane 4) upon irradiation of *N*-benzoyloxy pyridinethione

<p><b>1b</b> (4.45 mM in acetonitrile) for 3 h by a femtosecond laser at 775 nm; (lane 3) upon irradiation of <i>N</i>-benzyloxy pyridinethione <b>1e</b> by a femtosecond laser at 775 nm for 3 h; (lane 2) upon irradiation of <i>N</i>-hydroxy pyridinethione <b>1a</b>; and (lane 1) upon irradiation by a femtosecond laser at 775 nm for 3 h in the absence of any additive compound. ....</p>	52
<p>Figure 25. Gel electrophoresis analysis of pBR 322 DNA (0.5 µg/µL in 10 mM Tris-HCl 1.0 mM EDTA buffer, pH 8.0): (lane 5) upon irradiation of <i>N</i>-<i>t</i>-butoxy pyridinethione <b>1f</b> (4.45 mM in acetonitrile) for 3 h by a femtosecond laser at 775 nm; (lane 4) upon irradiation of <i>N</i>-benzoyloxy pyridinethione <b>1b</b> by a femtosecond laser at 775 nm for 3 h; (lane 3) upon irradiation of <i>N</i>-benzyloxy pyridinethione <b>1e</b>; (lane 2) upon irradiation of <i>N</i>-hydroxy pyridinethione <b>1a</b>; and (lane 1) upon irradiation by a femtosecond laser at 775 nm for 3 h in the absence of any additive compound.....</p>	54
<p>Figure 26. Gel electrophoresis analysis of strand breaks generated in pBR 322 DNA (0.5 µg/µL 10 mM Tris-HCl, pH 8.0, 1 mM EDTA) upon femtosecond irradiation of <i>N</i>-hydroxy pyridinethione <b>1a</b> for 30, 60, 90, 120 and 180 min at 775 nm corresponding to lanes 1-5 respectively. pBR 322 DNA (0.5 µg/µL 10 mM Tris-HCl, pH 8.0, 1 mM EDTA) with <b>1a</b> additive (4.45 mM in acetonitrile) not exposed to irradiation is shown in lane 6. ....</p>	58
<p>Figure 27. Results of time-dependent irradiation study using <i>N</i>-hydroxy pyridinethione <b>1a</b> (4.45 mM in acetonitrile) and buffered pBR 322 DNA (0.5 µg/µL 10 mM Tris-HCl, pH 8.0, 1 mM EDTA). Results are displayed graphically in a fraction of supercoiled DNA versus irradiation time plot. Line of best fit added from non-linear least squares regression.....</p>	60
<p>Figure 28. Structure of <i>N</i>-anthracenoyloxy pyridinethione <b>1g</b>.....</p>	64
<p>Figure 29. Absorption spectra of <i>N</i>-anthracenoyloxy pyridinethione <b>1g</b> (10<sup>-5</sup> M) in acetonitrile before and after exposure to room light for 1 min.....</p>	66
<p>Figure 30. Absorption spectra obtained, before irradiation of a solution of <i>N</i>-anthracenoyloxy pyridinethione <b>1g</b> in acetonitrile; after 775 nm femtosecond irradiation of <b>1g</b> solution at 20 min intervals (from 20 min to 160 min); after 775 nm femtosecond irradiation of <b>1g</b> solution for 360 min and after exposure of <b>1g</b> solution to room light for 5 min. Absorption spectra are presented sequentially in the order they were presented in</p>	



the caption, with the absorption spectra before irradiation of **1g** solution corresponding to the highest absorbance.....68

Figure 31. Relationship between absorption by a solution of *N*-anthracenoyloxypyridinethione **1g** in acetonitrile at 367 nm and corrected femtosecond irradiation time. Note that the final point is the absorbance after complete decomposition, and it was arbitrarily placed at 10<sup>4</sup> s. ....69

## ABSTRACT

DNA photocleaving reagents are a unique class of molecules that display the ability to cleave DNA, causing strand breaks, upon exposure to an irradiation source. In terms of biological applications, achieving excitation through a two-photon absorption event provides for unique benefits that can be useful in such applications as photodynamic therapy and cell viability studies. Thus, this thesis pertains to the study of a class of photocleaving reagents that have been shown to become excited through a two-photon process during irradiation with a pulsed femtosecond laser at 775 nm.

*N*-(Alkoxy)pyridinethiones were selected as possible oxygen-based radical generators upon irradiation at two-photon wavelengths. Experiments were carried out with pBR 322 plasmid DNA to determine if these *N*-(alkoxy)pyridinethiones could cause strand cleavage and if so how efficient they are in doing so. Several compounds were found to be effective DNA strand cleavers when irradiated at two-photon wavelengths, displaying the utility of two-photon excitation in biological studies. Rationale is suggested for the observed variation in cleaving efficiency based on inherent properties of the generated radicals.

A second study was done to measure the two-photon cross section of the compound *N*-(anthracenoyloxy)pyridinethione. The two-photon cross section was found by measuring the fraction of substrate remaining after specific periods of femtosecond laser irradiation at 775 nm, and the two-photon cross section was found to be 0.051 GM.

## LIST OF ABBREVIATIONS USED

1PA	One-photon absorption
2PA	Two-photon absorption
2PE-PDT	Two-photon excited photo-dynamic therapy
3D	Three-dimensional
A	Adenine
AMD	Age-related macular degeneration
AP site	Apurinic/apyrimidic site
APCI	Atmospheric-pressure chemical ionization
Ar·	Aroyloxy radical
bp	Base pair
C	Cytosine
DCM	Dichloromethane
DMAP	4-Dimethylaminopyridine
DMF	Dimethylformamide
DNA	Deoxyribonucleic acid
EDTA	Ethylenediaminetetraacetic acid
ESI	Electrospray ionization
F	Photon flux
G	Guanine
GM	$10^{-50} \text{cm}^4/\text{s}/\text{photon}$ (Goeppert-Mayer cross section)
High-res	High resolution
h $\nu$	Light
I	Intensity of irradiation
IR	Infrared
k	Rate constant
Low-res	Low resolution
M <sup>+</sup>	Molecular ion
MS	Mass spectrometry
N <sub>GS</sub>	Number of molecules in ground state

NMR	Nuclear magnetic resonance
$N_{OP}$	Number of molecules in the excited state due to 1PA
$N_{TP}$	Number of molecules in the excited state due to 2PA
PDT	Photo-dynamic therapy
PMT	Photo-multiplier tube
ppm	Parts per million
ps	Picoseconds
$PsY\cdot$	2-Pyridylthiyl radical
R	Correlation coefficient
RNA	Ribonucleic acid
ROS	Reactive oxygen species
$S_0$	Ground state
$S_1$	Lowest singlet excited state
$S_2$	Excited singlet state
$S_n$	n'th excited singlet state
SSBs	Single strand breaks
T	Thymine
TAE	Tris-acetate-EDTA buffer
Ti:sapphire	Titanium:sapphire
TLC	Thin-layer chromatography
TMS	Trimethylsilyl
TPEF	Two-photon excited fluorescence
UV	Ultra-violet
$\gamma$	Gamma
$\delta$	Two-photon cross section
$\eta$	Fluorescence quantum yield
$\lambda$	Wavelength
$\sigma$	One-photon cross section

## ACKNOWLEDGEMENTS

I would like to take this opportunity to thank the numerous people that have helped and supported me over the past two years as I did my research work and prepared this thesis in pursuit of my master's degree.

Firstly, I would like to thank my research supervisor Dr. Norman P. Schepp for providing me this wonderful opportunity and allowing me to participate in his unique research. His guidance and advice have led me through the past two years and made this whole thing possible. Under his tutelage I feel like have learned an invaluable amount of knowledge about research and chemistry, and for this I sincerely thank him.

I would also like to thank my supervisory committee members Dr. Frances L. Cozens and Dr. Robert L. White. Aside from serving on my committee, I would like to thank Dr. Cozens for answering my questions and providing advice whenever I have needed it over the years. I would also like to thank Dr. White for being a very influential figure in my life, guiding me through completion of my undergraduate degree, helping me with my medical school endeavors, and always being there when I needed him for anything.

In terms of help from around the department I have found it in so many places and could thank an endless amount of people here, but I would like to take this chance to mention a few individuals. Thanks to Dr. Mike Lumsden for his help with the NMR facilities and a big thanks to Mr. Xiao Feng for the many mass spectra he provided for me. Thanks to Dr. D. Jean Burnell for answering all my questions and his assistance with my medical school applications. And lastly thank you to Dr. Reinaldo Moya Barrios for guiding me through the teaching assistance requirement of this degree.

I would like to thank the whole Schepp and Cozens research group for making this past two years the best it could be. This includes all the undergraduates and summer students who have been in and out of the lab over the years; everyone in the group played a part in this no matter how large or small and I thank them all. A special thanks goes out to Duncan Halverson-Smith for providing some of the background work for this project.

I would like to say a huge thank you to my parents for standing by me with endless support and love throughout this process. None of this would have ever happened without them and I thank them 1000 times over for this opportunity, love you guys.

Also I would like to say a huge thanks to my girlfriend, Alexandra Baker, for being so patient over these two long years. She has provided the support and most importantly the inspiration and motivation that has driven me through this degree and into my future endeavors. Thanks so much, love you.

Lastly, I would like to thank the whole Dalhousie Department of Chemistry from the office staff to fellow students they have all made this time here wonderful and helped me through this process, thanks everyone.

## Chapter 1 Introduction

### 1. Two-Photon Absorption

#### 1.1 Two-photon Absorption: Introduction

Two-photon absorption (2PA) represents the excitation of a molecule from one electronic state (most commonly ground) to a higher electronic state *via* the absorption of two photons of identical or differing frequencies. Dr. Maria Goeppert-Mayer<sup>[1]</sup> first hypothesized this phenomenon in 1931 in her doctoral dissertation at the Göttingen University in Germany. The theory remained unproven until the subsequent invention of the ruby laser thirty years later.<sup>[2]</sup> The ruby laser was able to produce intensities high enough for 2PA to occur, and experimental verification of this phenomenon was provided when two-photon excited fluorescence was detected in europium-doped crystal by Kaiser and Garrett.<sup>[3]</sup> Shortly thereafter, Peticolas, Goldsborough and Reickhoff showed 2PA in a variety of organic crystals and solutions,<sup>[4,5]</sup> laying the groundwork for further exploration into this phenomenon. 2PA became significantly easier to investigate as sub-picosecond pulsed lasers became more readily available in the 1990s (particularly the Ti:sapphire laser),<sup>[6]</sup> and has been extensively studied for the last 20+ years.

The applications of 2PA were demonstrated for the first time by Rentzepis in optical data storage<sup>[7]</sup> and Webb in microscopy<sup>[8]</sup> in 1989 and 1990 respectively. However, the scope of 2PA applications was limited in these early days by the relatively small two-photon cross sections (that is, the ability of an atom or molecule to absorb light at a specific wavelength through a 2PA event (*vide infra*)) of molecules known at the

time. Subsequently, there was an extensive effort put forth to further understand, both theoretically and experimentally, the structure-property relationships for 2PA chromophores, and a significant number of new organic chromophores with enhanced two-photon cross sections have been developed.<sup>[6]</sup> Over the past two decades from the 1990s to date, two-photon absorbing molecules have been widely applied in both material and biological sciences. The major applications in material science include three-dimensional (3D) optical data storage,<sup>[9,10]</sup> microfabrication and lithography,<sup>[11]</sup> up-converted lasing,<sup>[12]</sup> optical power limiting,<sup>[13]</sup> and two-photon excited microscopy.<sup>[14-18]</sup> Most recently 2PA has seen a surge in interest with biologically related applications namely in two-photon excitation photodynamic therapy,<sup>[19]</sup> two-photon photoliberation of active substances<sup>[20]</sup> and O<sub>2</sub> sensing.<sup>[21]</sup>

### *1.1.1 Two-photon Absorption: Optic Fundamentals*

The simple schematic of an energy diagram, Figure 1, will be referenced throughout this chapter as an aid in explaining 2PA.



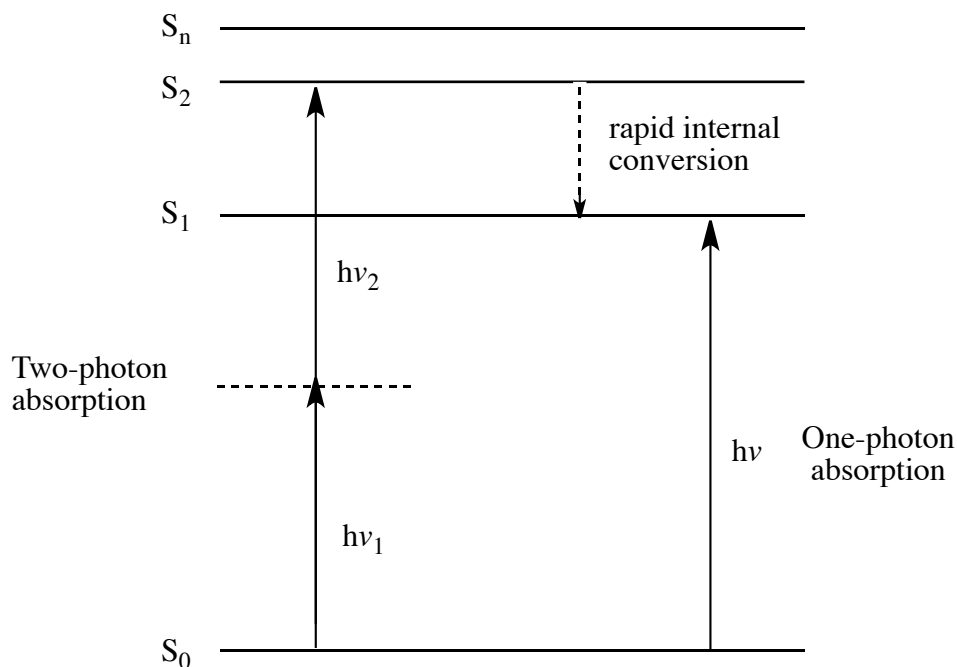


Figure 1. Energy diagram depicting one- and two-photon absorption.

In one-photon absorption (1PA), excitation from the ground state ( $S_0$ ) to an excited state ( $S_1$ ) involves the absorption of a single photon,  $h\nu$ , with an energy that matches the energy difference between the two states. In 2PA, an excited state (for example  $S_2$  in Figure 1) is reached using two photons,  $h\nu_1$  and  $h\nu_2$ . As individual entities neither of these photons possesses the energy necessary to achieve an excited state, yet when the energies of the two photons are summed, promotion to an excited state can be achieved. The dotted line in Figure 1 represents a virtual state (not a true eigenstate state) created when the first photon is absorbed. This virtual state exists for a very short time of a few femtoseconds ( $10^{-15}$ sec). If absorption of a second photon occurs within this small window the molecule is excited to a longer lived excited state, such as the  $S_2$  state. Since the second photon must be absorbed so quickly after the first photon is used to reach the extremely short-lived virtual excited state, this kind of absorption is called "simultaneous" 2PA. It differs from a "step-wise" two-photon process in which the first photon is used to

excited the molecule to a stable excited state (e.g. usually  $S_1$ ) and then the second photon is used to excite the molecule to a higher excited state. In step-wise two-photon excitation, a substantial amount of time can pass before the second photon is added since the  $S_1$  state is normally relatively long-lived ( $\approx 10^{-9}$  s). Once in an excited state the molecule will quickly relax to the lowest excited state,  $S_1$ . From the  $S_1$  state the system can return to the ground state ( $S_0$ ) through the emission of fluorescence or by non-radiative decay. Various alternative events are possible from  $S_1$ , including intersystem crossing from singlet to triplet state, as well as chemical reactions from the  $S_1$  state.

A rate equation can be written for the formation of an excited state in a molecule *via* one-photon absorption (1PA) as seen below in eq. 1.1,

$$\frac{dN_{OP}}{dt} = \sigma N_{GS} F \quad (1.1)$$

where  $\sigma$  is the one-photon absorption cross section,  $N_{GS}$  is the number of molecules per unit volume in the ground state,  $N_{OP}$  is the number of molecules in the excited state due to 1PA,  $F$  is the photon flux and  $t$  is time.

Eq. 1.1 shows that the number of molecules promoted to an excited state *via* 1PA ( $N_{OP}$ ) has a linear relationship with photon flux (equivalent to incident light intensity,  $I$ ), as well as a linear relationship with the number of molecules in ground state ( $N_{GS}$ ). As well, eq. 1.1 clearly shows that the one-photon cross section,  $\sigma$ , will dictate the probability of an absorption event occurring, with a typical value for a one-photon cross section being  $\sigma = 1.0 \times 10^{-17} \text{ cm}^2/\text{photon}$ .

A rate equation for 2PA can be written as eq. 1.2,

$$\frac{dN_{TP}}{dt} = \frac{1}{2} \delta N_{GS} F^2 \quad (1.2)$$

where  $\delta$  is the two-photon absorption cross section and  $N_{TP}$  is the number of molecules per unit volume in the excited state due to 2PA. Eq. 1.2 shows that 2PA has a quadratic, or non-linear, relationship with photon flux  $F$ , while maintaining a linear relationship with the number of molecules in the ground state,  $N_{GS}$ . As previously mentioned photon flux is proportional to the intensity of incident light ( $I$ ) and therefore it is commonly stated that efficiency of 2PA has a quadratic relationship with the intensity of incident light or is proportional to  $I^2$ . This non-linear relationship with intensity is the basis of applications involving 2PA. Eq. 1.2 also shows that that the probability of a two-photon event occurring depends on the two-photon cross section,  $\delta$ . Values of  $\delta$  are in the  $\delta = 1.0 \times 10^{-50} \text{ cm}^4\text{s}/\text{photon}$  range, and are significantly smaller than those for a typical one-photon cross section. This large difference between two-photon and one-photon cross sections gives rise to the comparatively weak ability of molecules to participate in a 2PA event compare to that of a 1PA event.

### *1.1.2 Two-Photon Absorption: Applications*

There are several characteristics of 2PA that allow for its applications. The characteristics that apply to the interests of this thesis (biological applications) include deeper penetration into biological tissue with near-infrared (IR) light that is typically used for 2PA, and spatially selective excitation of molecules in a small volume around the focal point of the irradiating laser beam. As previously mentioned these characteristics are fundamentally derived from the quadratic dependency of 2PA on incident light intensity. These advantageous characteristics of 2PA are described in the following

paragraphs with the point of not only demonstrating function, but also displaying how 2PA can be favorable when directly compared to 1PA.

Since in 2PA the energies of the two photons absorbed are added up, the excitation wavelength is typically significantly longer than that used for 1PA. 2PA wavelengths are typically in the region of red to near-IR light (600-800 nm), while typical 1PA wavelengths are in the region of ultra-violet (UV) light (300-400 nm). Because the photon energy in 2PA is well below that at which the medium absorbs *via* 1PA, it is possible using near-IR light to excite molecules at an increased depth, relative to UV excitation, in a high-absorbing medium. Figure 2, based on experimental results published by Marder *et al.*,<sup>[22]</sup> displays results from an experiment that shows the deeper penetration capabilities of 2PA wavelengths.<sup>[22]</sup>

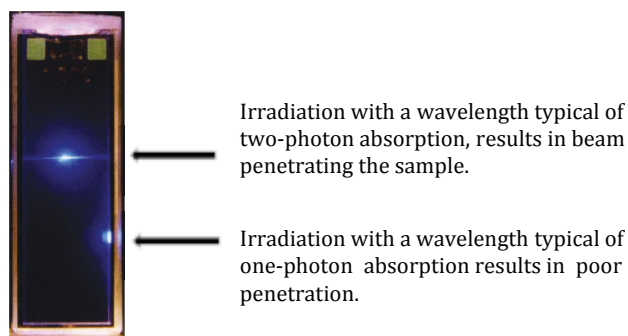


Figure 2. Fluorescence from a concentrated solution of a fluorophore using (TOP) two-photon excitation and (BOTTOM) one-photon excitation. Taken from ref. 22 (*use of picture granted by copyright holder*).

Shown in Figure 2 is a cell containing a relatively high concentration of a fluorescent compound that readily absorbs at both one and two-photon wavelengths. Two light beams are directed toward the cell from right to left with wavelengths appropriate for 2PA (upper beam) and 1PA (lower beam). It can be seen that with 1PA wavelengths,

fluorescence emission (represented by bright spot) is only present close to the wall of the cell on the side the beam is focused on. This is because the beam is strongly absorbed, making its penetration minimal. It is also shown that with wavelengths appropriate for 2PA, fluorescence is achieved from the fluorophore in the centre of the cell. This is because 2PA, and thus the observed fluorescence, only takes place at the focal point where the intensity of the laser is sufficiently high, and is therefore able to penetrate the sample. Typical chromophores used in biological studies absorb in the UV region *via* 1PA. When using near-IR irradiation deeper penetration into biological tissue can be achieved, as the photons will not be absorbed by the other chromophores present in biological medias due too insufficient energy, analogous to the experiment in Figure 2. This allows for excitation of photoreagents significantly deeper within tissue.

The use of near-IR light typical of 2PA is also less toxic toward biological tissue then UV light. In humans, prolonged exposure to UV radiation may result in chronic health effects on the skin, eyes, and immune system.<sup>[23]</sup> Moreover, UV light is known to cause DNA damage that can lead mutagenesis or carcinogenesis (*vide infra*).<sup>[23]</sup> Such health risks are not associated with near-IR light, and therefore use of lower energy light required for 2PA can be significantly less toxic toward biological tissue, limiting collateral damage to neighboring tissue when used as a therapeutic excitation source (section 2.1.2.2).

When laser light is focused in a two-photon absorbing medium at the diffraction-limit, 2PA is effectively confined to a small focal volume. This characteristic allows for spatially controlled “pinpoint” excitation of molecules.<sup>[22]</sup> Figure 3 displays a experiment

showing the enhanced spatial control that can be achieved with a focused laser beam at 2PA wavelengths.<sup>[22]</sup>

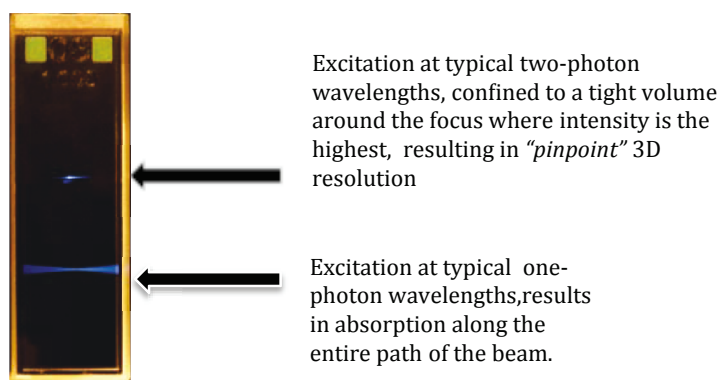


Figure 3. Fluorescence from a dilute solution of a fluorophore using (TOP beam) two-photon excitation and (BOTTOM beam) one-photon excitation. Taken from ref. 22 (*use of picture granted by copyright holder*).

In Figure 3 a fluorescent compound that readily undergoes both one- and two-photon absorption is contained within a cell. Two light beams are propagated through the cell from right to left with wavelengths appropriate for 2PA (upper beam) and 1PA (lower beam). At wavelengths appropriate for 1PA, molecules are excited throughout the beam path, shown as fluorescence emission (bright area) across the cell. At wavelengths appropriate for 2PA only molecules very close to the focal point of the beam are excited, shown as fluorescence emission in the center of the cell where the beam has been focused. The smaller excitation volume of a focused laser at 2PA wavelengths is based on the rate at which beam intensity decreases as you move away from the focus. The decrease of beam intensity will effect 2PA at a rate which is double that of 1PA, as 2PA is proportional to  $I^2$ , while 1PA is proportional to  $I$ . The ability to spatially control and confine the excitation volume of molecules excited through 2PA is used to optimize biological applications such as photodynamic therapy and photoliberation of active

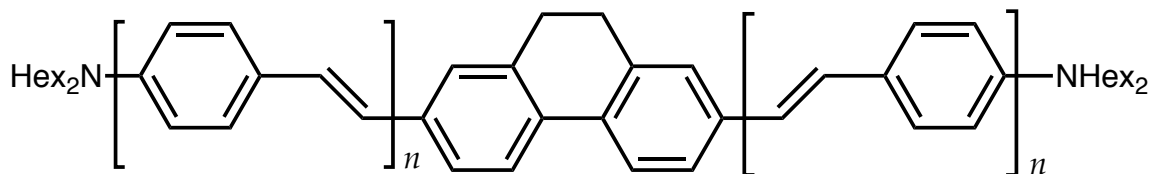
substances. Greater spatial control allows for activation of photoreagents to be achieved more selectively within tissue while minimizing collateral damage to surrounding tissue (section 2.1.2.2).

### *1.1.3 Two-photon Absorption: Cross Section*

As seen in eq. 1.2 the two-photon cross section,  $\delta$ , represents the ability of a given atom or to molecule absorb light at a specified wavelength through a 2PA event. 2PA cross sections are usually reported in the units of GM's (Goeppert-Mayer, 1 GM =  $10^{50}$  cm<sup>4</sup>s/photon). These units result from the product of two areas (one for each photon, both in cm<sup>2</sup>) and a time (within which the two photons must arrive to achieve 2PA). The large scaling factor evident in the GM unit is used to give convenient values for two-photon cross sections of most common dyes.

To some extent, linear and non-linear absorption strength are related, and therefore the first compounds investigated for 2PA efficiency were laser dyes. However, these dyes were found to have low or moderate experimental two-photon cross sections on the order of  $\delta = 0.1$ -10 GM. It was not until the 1990's that the rational design of two-photon absorbing molecules began to be developed, in response to a need from imaging and data storage technologies.<sup>[24]</sup> Some general features that were found to enhance 2PA cross sections are extended conjugation length of  $\pi$ -bridge, molecular planarity, and donor/acceptor models.<sup>[24]</sup> Delocalization of electrons, achieved from the general features mentioned above, will decrease the band gap between the highest occupied molecular orbital and lowest occupied molecular orbital, thus lowering the energy required for a 2PA event smaller. The compounds<sup>[25]</sup> shown in Figure 4 exemplify some features of

chromophores developed with enhanced 2PA cross sections. For  $n = 1$ , this material has extended conjugation and has a large 2PA cross section of 1700 GM (with 740 nm excitation).<sup>[25]</sup> When the conjugation is further extended as for  $n = 2$ , the 2PA cross section increases to 3400 GM.<sup>[25]</sup> Another feature that can be noted is the use of a donor-acceptor model. The electron donor in this case is the dialkyl amino group,  $\text{NHex}_2$ , and the acceptor is the electron deficient fused diaryl group at the center of the molecule. The final feature that can be noted is the rigidity or planarity of this molecule, which is achieved by fusing the aryl groups to limit rotation. All of these features decrease the band gap, lowering the energy needed for 2PA to occur, and in turn making a 2PA event more likely.



$$n = 1, \delta = 1700 \text{ GM at } 740 \text{ nm}$$

$$n = 2, \delta = 3300 \text{ GM at } 740 \text{ nm}$$

Figure 4. Structures of chromophores<sup>[25]</sup> that exemplify general structural features for 2PA enhancements.

### 1.1.3.1 Two-photon Absorption: Cross Sections- Measurements

A common technique used for measuring 2PA cross sections is two-photon excited fluorescence (TPEF). One alternative technique, used in the present work,



monitors the photodecomposition of the two-photon absorbing chromophore using absorption spectroscopy as a function of irradiation time (Chapter 4).

#### *1.1.3.1.1 Two-photon Excited Fluorescence (TPEF)*

Intensity of TPEF provides direct information on the efficiency of 2PA.

Numerous variants of this experiment have been developed since it was first reported by Xu and Webb.<sup>[26]</sup> 2PA cross sections can be measured in two ways with this technique, absolute or relative. A relative measurement, which is the simplest case and often employed, can be taken if a suitable reference compound is available with a known 2PA spectrum. In this approach the one and two-photon excited fluorescence excitation spectra of the sample and the reference sample are compared under identical conditions. This double-referencing method allows for a large number of variables not to be considered. For a relative measurement it is not necessary to know parameters relating to the excitation light (pulse energy, pulse duration, and temporal intensity distribution), the wavelength dependence of the efficiency of the detector, nor the concentration and fluorescence quantum yield of the sample.<sup>[27]</sup> This makes relative measurements particularly favorable compared to absolute, in which all these parameters must be measured individually. The TPEF technique has been optimized extensively by Rebane, Drobizhev and co-workers,<sup>[27]</sup> and this group has recently reported accurate reference 2PA spectra for a wide range of commercially available dyes, making the TPEF method an attractive option.<sup>[28]</sup>

Figure 5 displays a basic schematic of this technique. In Figure 5 the laser beam is propagated through the material of interest, and fluorescent light is then emitted after

the molecules in the material become excited. This fluorescence emission is collected and measured with a detector, such as a photomultiplier tube (PMT).

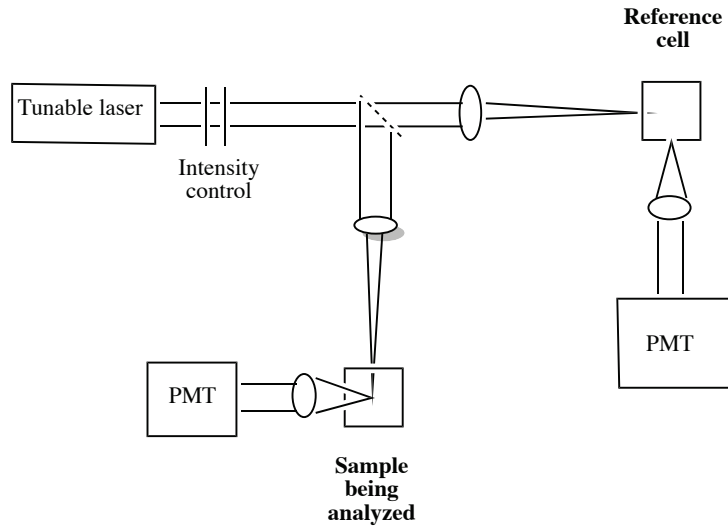


Figure 5. Schematic of the setup for a two-photon induced fluorescence experiment.

The number of molecules excited by 2PA per unit time and volume,  $N_{TP}$ , is proportional to the two-photon cross section of the material at that given excitation wavelength, molecular concentration and the square of photon flux. The number of fluorescent photons emitted by these molecules,  $N_{fl}$  is then represented by eq. 1.3:

$$n_{fl} = \eta N_{TP} \quad (1.3)$$

where  $\eta$  represents the fluorescence quantum yield of the material. From this we can look back to equation 1.2 (p. 5) to determine that the intensity of two-photon induced fluorescence is proportional to the two-photon cross section,  $\delta$ , and a measurement can be recorded.

#### *1.1.4 Two-Photon Absorption: Laser as a Light Source*

The name laser is an acronym for “light amplification by stimulated emission of radiation.”<sup>[29]</sup> Laser light is characterized by being monochromatic, coherent and concentrated. Being monochromatic implies that the laser light consists of only one wavelength, or a very narrow range of wavelengths. This is very different from conventional light emitted from a light bulb, which emits over a much broader range of wavelengths. For example, most incandescent light bulbs emit over the whole visible spectrum and some of the infrared spectrum. The second unique ability of a laser is its ability to emit light waves in phase, which is known as coherence. The spatial coherence of the laser beam allows for it to be focused on a tight spot.

Ultra-short pulsed lasers are a specific laser class that can be used to achieve 2PA. They are characterized as lasers that provide pulses of light with time durations on the order of femtoseconds ( $10^{-15}$  seconds); this generates the very high instantaneous photon densities that are necessary in achieving any significant 2PA.

## Chapter 2 Radicals in Biological Systems

### 2. Free Radicals: Oxidation of Biological Molecules

#### 2.1 Free Radicals: Formation

A free radical is defined as: “a reactive chemical species having a single unpaired electron in an outer orbit.”<sup>[30]</sup> They are often formed through the homolysis of covalent bonds, Figure 6.



Figure 6. Homolytic bond cleavage resulting in radical formation.

For biological/biochemistry studies, radicals have been generated by several methods, often with the aim of generating hydroxyl ( $\cdot\text{OH}$ ) radicals. The classical approach to  $\cdot\text{OH}$  radical generation can be taken, which involves chemical formation through the Fenton reaction,<sup>[31]</sup> or the  $\gamma$  radiolysis of water.<sup>[32]</sup> Yet, these classical  $\cdot\text{OH}$  radical sources are limited in scope for biological investigations. The Fenton reaction may initiate unwanted redox chemistry and is limited to  $\cdot\text{OH}$  radical production, while  $\gamma$  radiolysis, also limited to  $\cdot\text{OH}$  radical production, may cause direct ionization of DNA. In more recent studies, photochemical generation of radicals has been used in biological/biochemistry investigations<sup>[33-40]</sup> as a more versatile approach allowing for a wider variety of radicals to be generated, while minimizing direct damage to DNA (photochemical radical generation discussed further in section 2.1.2).

### 2.1.1 Free Radicals: Oxidative Damage to DNA

Aerobic living organisms continuously produce free radicals by normal intracellular metabolism; normal production plays an important role in biological function. However, free radicals, which are highly reactive, can also be very harmful to cells through the oxidation of biomolecules. Oxidizing biomolecules, such as nucleic acids (section 2.1.1.1), proteins and lipids, can cause a range of damage on a cellular level from loss of specific cell function to cell death, while on a macro-cellular level have been implicated in a number medical conditions (*vide infra*). Free radicals become harmful when uncontrolled production is initiated by an exogenous source and the cellular defense mechanisms are overcome and fail. Examples of exogenous agents include ionizing radiation, ultra-violet (UV) radiation, redox-cycling drugs and environmental pollutants.<sup>[41]</sup> Substantial evidence has been accumulated regarding the importance of oxidative damage to biomolecules (oxidative stress)<sup>[42,43]</sup> in several medical conditions including inflammation,<sup>[44]</sup> aging,<sup>[45-47]</sup> mutagenesis, carcinogenesis,<sup>[42,48]</sup> and also in human immunodeficiency virus expression.<sup>[49]</sup> Although exogenously induced radicals can be highly destructive, they can also serve a positive function as outlined below and further in the photodynamic therapy section. As well, their study can provide insight into how these radicals interact with biomolecules thereby furthering our understanding of radical chemistry in biological systems.

### 2.1.1.1 Free Radicals: Mechanisms of Oxidative DNA Damage

Oxidation of DNA can result in damage to all four nucleobases [adenine (A), guanine (G), cytosine (C), thymine (T)] as well the deoxyribose sugar moiety. Figure 7 displays the structure of a nucleotide with the individual moieties highlighted.

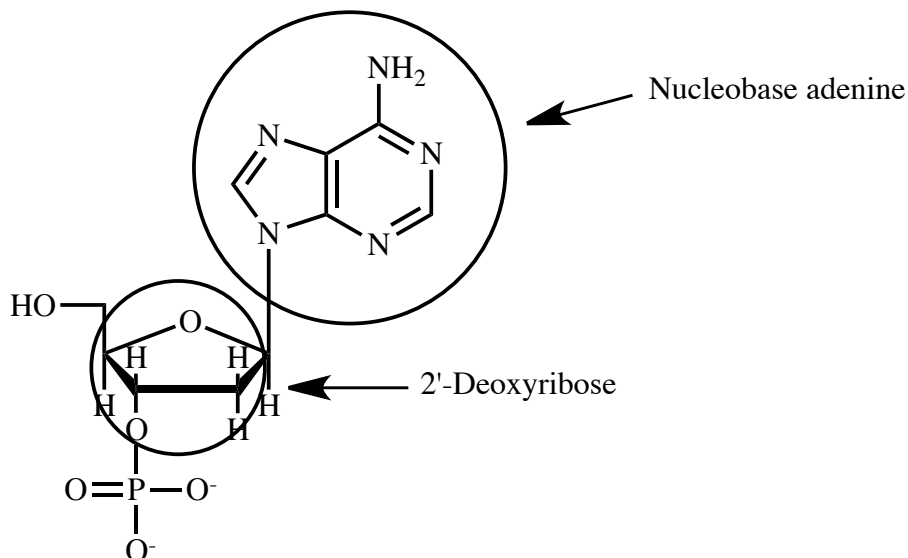


Figure 7. Structure of a nucleotide, with the nucleobase and 2'-deoxyribose sugar moieties highlighted. It should be noted that an adenine base is used in this structure but any of the other three nucleobases can appear in this position linked with a nitrogen-carbon bond.

The oxidation of DNA induced by reaction with  $\cdot\text{OH}$  radicals has been extensively documented.<sup>[36,38,41,50-52]</sup> Two prominent pathways by which  $\cdot\text{OH}$  radicals are known to create DNA damage have been proposed: addition of the  $\cdot\text{OH}$  radicals to bases, causing base modifications, and direct hydrogen abstraction by  $\cdot\text{OH}$  radicals from the deoxyribose sugar moiety in the DNA backbone. It should be noted that other

mechanisms by which  $\cdot\text{OH}$  radicals damage DNA have been proposed, such as electron transfer and hydrated electrons.<sup>[41]</sup>

Damage to DNA bases occurs when  $\cdot\text{OH}$  radicals undergo addition reactions adding to the double bonds of heterocyclic DNA bases, shown in Figure 8. This is known as base modification, which damages the genome, giving rise to oxidized bases, AP sites (DNA that is neither purine or pyrimidine base), and DNA strand breaks.<sup>[41]</sup>

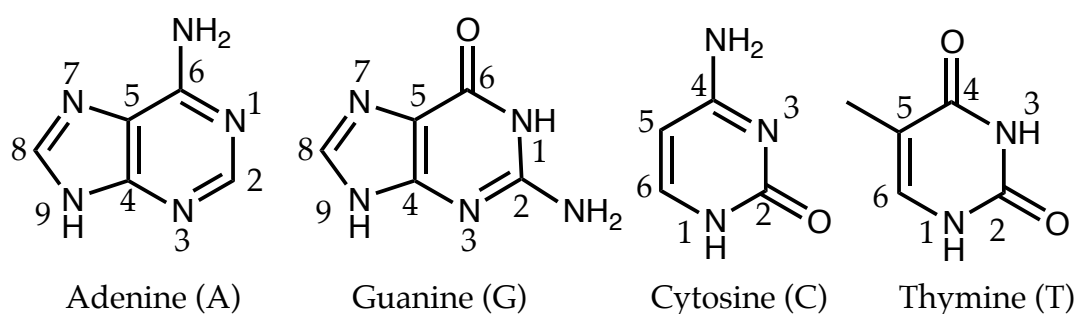


Figure 8. DNA bases with ring positions numbered.

Among the DNA base pairs, guanine has the lowest reduction potential at 1.29 V, and as a result it is the best electron donor and is preferentially oxidized over the other base residues.<sup>[41]</sup> Because oxidation is mostly likely to occur on the guanine residue, this base residue has been used to provide an example of addition. Thus, Figure 9 displays possible  $\cdot\text{OH}$  radical reactions with a guanine residue, with the radical adding at C2-, C4-, C5-, or C8- positions of the heterocyclic ring forming OH-adduct radicals. Figure 9 also displays a less likely  $\cdot\text{OH}$  radical abstraction reaction from a guanine residue forming a nitrogen-centered radical; thymine is the only other base that undergoes hydrogen abstraction at the C5- methyl group.

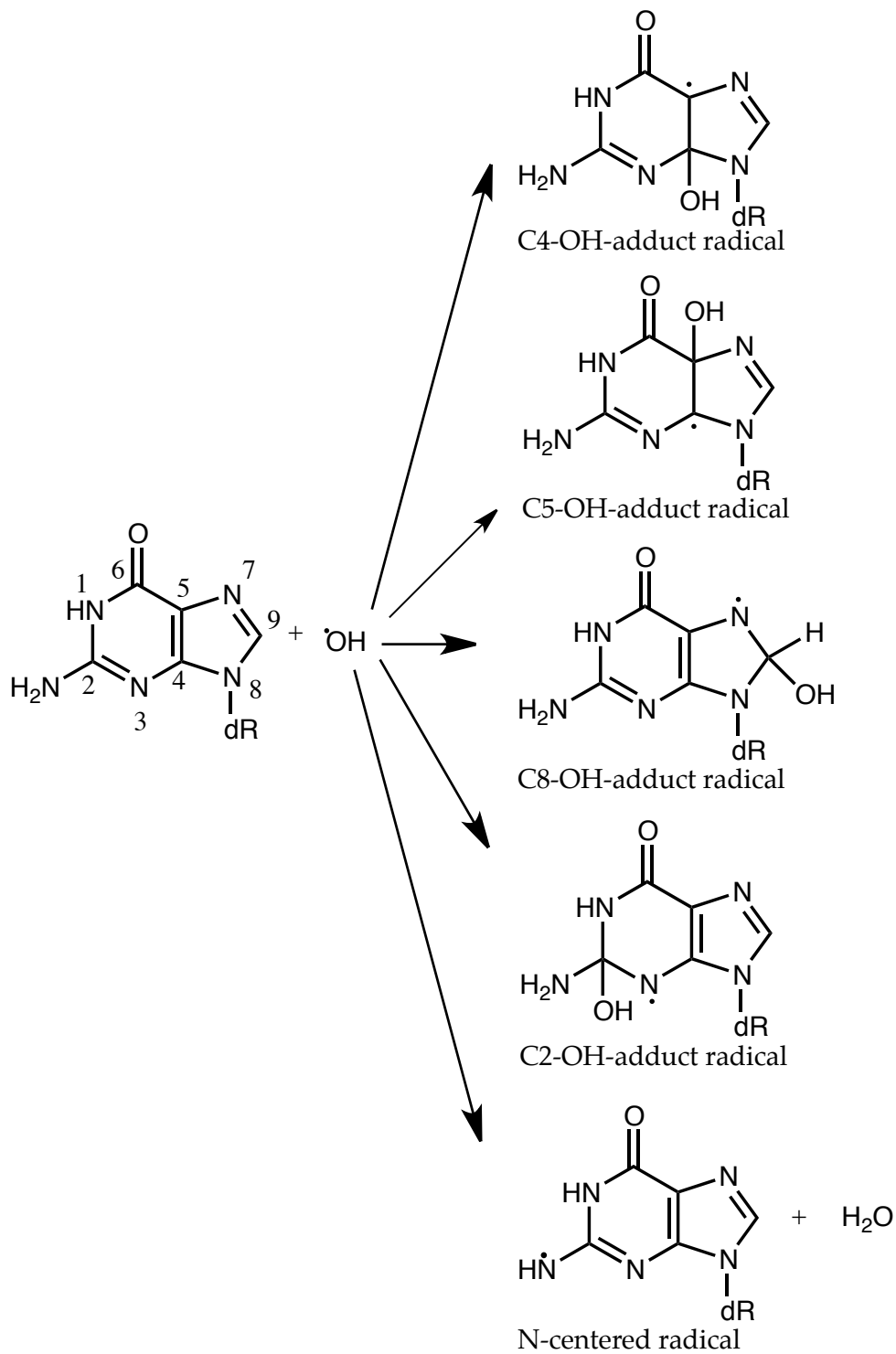


Figure 9. Products of  $\cdot\text{OH}$  radical addition (OH-adducts) and abstraction (N-centered radical) from a guanine base.



$\cdot\text{OH}$  radical addition reactions normally occur at the C4-, C5- and C8- positions of purine bases (guanine and adenine), as well as adding across the C5-C6 double bond of pyrimidines (cytosine and thymine). The reaction pathways taken after  $\cdot\text{OH}$  radical addition occurs are fairly complex; for the purpose of this thesis it is enough to say that they result in DNA damage, which in many cases cause DNA strand breaks. Base modifications and their consequences have been reviewed by Aust and Eveleigh,<sup>[50]</sup> as well as Dizdaroglu *et al.*<sup>[51]</sup>

Hydrogen abstraction occurs primarily from one of the five carbon atoms of 2'-deoxyribose sugar moiety, shown in Figure 10. It can also occur from the methyl group on thymine and to a lesser extent from the C2- position of guanine, as mentioned above.

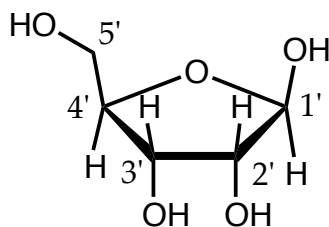
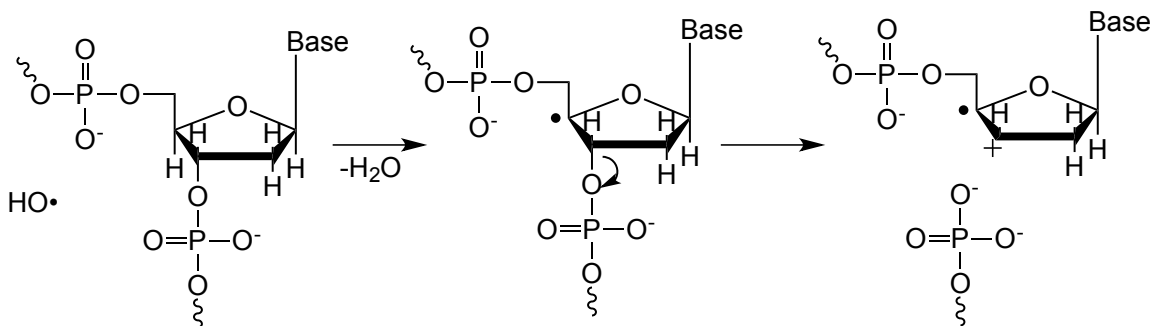


Figure 10. 2'-Deoxyribose sugar with labeled positions.

Hydrogen abstraction reactions form carbon-centered radicals at the five-labeled carbon-positions (1' to 5') in Figure 10. Abstraction from the deoxyribose sugar can lead directly to DNA strand breaks. This is the most severe form of DNA lesion, with the highest chance of causing permanent mutations. Scheme 1 outlines a reaction mechanism, by which the carbon-centered radical on a deoxyribose sugar can further react to give strand cleavage. In Scheme 1 a carbon centered radical is formed at C4' by hydrogen abstraction using  $\cdot\text{OH}$  radical. This enhances the leaving group ability of appropriate

neighboring groups,<sup>[53]</sup> which in this case results in rapid ionization of the phosphate group at C3' and DNA strand cleavage.<sup>[53]</sup>

**Scheme 1.** DNA strand cleavage following hydrogen abstraction by a  $\cdot\text{OH}$  radical at the C4'- of deoxyribose.<sup>[53]</sup>



### 2.1.2 Free Radicals: DNA Photocleaving Reagents

The design of biologically functional molecules has been a foremost research goal of chemistry, biology, and medicine, covering such topics as catalysis, drug design, host-guest interactions, catalytic antibodies and synthetic enzymes.<sup>[54]</sup> The topic of synthetic enzymes, among others, involves research that is focused on the development of nucleolytic reagents that interact with DNA/RNA in order to ultimately cleave the phosphodiester backbone.<sup>[55]</sup> This class of reagents, commonly referred to as “artificial nucleases”, show great potential as a tool in molecular biology<sup>[56-58]</sup> and as possible chemotherapeutic agents for cancer or antiviral treatment.<sup>[59,60]</sup> Additionally, these reagents could be attached to selective carriers producing artificial restriction enzymes and specific gene-targeted drugs.<sup>[61,62]</sup>

The challenge that is faced in designing these artificial nucleases arises from the selection of a suitable chemical moiety that, when activated, will generate a reactive species able to damage and cleave nucleic acids. In this research, oxygen-based radicals have appeared as a potential candidate, since they are typically highly reactive and are known to have many biological functions.<sup>[43,63,64]</sup> Initially, oxygen-based radicals were generated in biological systems by redox chemistry and organometallic reagents using Cu(II),<sup>[65]</sup> Fe(II),<sup>[66,67]</sup> Co(II)<sup>[68]</sup> and Ni(II)<sup>[69]</sup> complexes. Despite seeing good use over the years, metal catalyzed methods of radical production suffer from practical limitations. Some of these limitations include the sensitivity of organometallic reagents to the presence of numerous biological species, such as glycerol, thiols, or metal ions. As well they require very high concentrations of chemical initiators, and are often limited in function to the formation of  $\cdot\text{OH}$  radicals.<sup>[54]</sup>

The search for an alternative, hopefully more efficient, nucleolytic reagent guided several groups toward the investigation of light-induced activation. This method is seen as advantageous as the cleavage is initiated using light, eliminating the need for an external chemical initiator. These photoactivated reagents, commonly called “photonucleases”, include complexes of Ru and Rh,<sup>[70]</sup> uranyl salts<sup>[71]</sup> and even the simplest method of just UV-light irradiation.<sup>[72]</sup> However all of these suffer from serious drawbacks, most notably relating to high reagent concentration needed, the high wavelength and intensity of the irradiation source, as well as the low quantum yields of the photoinitiation step.

The use of organic (non-metal) compounds is a relatively new approach to producing artificial nucleases and is yet to be extensively explored.<sup>[73-75]</sup> Such compounds

could undoubtedly display a different, perhaps unique reaction profile, and could be valuable assets in expanding and/or complementing the current repertoire of already established DNA/RNA cleaving agents. Over the past 15 years organic compounds have gained more traction in this field and various groups, including work done in this thesis, have reported purely organic light-activated compounds to have a significant DNA damaging profile.<sup>[34-38,40,52,55]</sup> One such class of compounds that has become the interest of several groups, including Schepp and colleagues,<sup>[76,77]</sup> are *N*-alkoxy pyridinethiones, with the general structure shown in Figure 11.

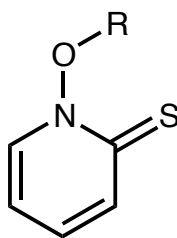


Figure 11. General structure of *N*-alkoxy pyridinethiones.

#### 2.1.2.1 Free Radicals: Photoradical Generators *N*-alkoxy pyridinethiones

UV-excitation of *N*-hydroxy pyridinethione, Figure 12, is a known method for the production of  $\cdot\text{OH}$  radicals.<sup>[78-80]</sup>

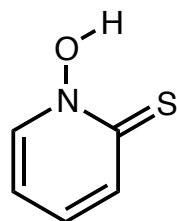


Figure 12. Structure of *N*-hydroxy pyridinethione.

*N*-Hydroxypyridinethione is a known antimicrobial, anticancer and antifungal agent;<sup>[81-83]</sup> its zinc and sodium salt forms are also used industrially in antidandruff shampoos.<sup>[84]</sup> *N*-Hydroxypyridinethione is also used as a precursor for *N*-alkoxypyridinethiones, Figure 11, and more specifically Barton esters (*N*-acyloxypyridinethiones), Figure 13.

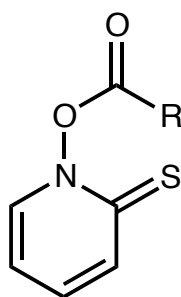


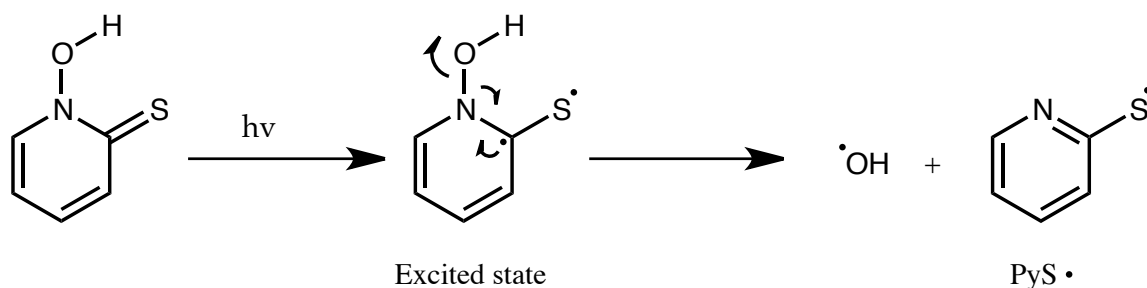
Figure 13. General structure of Barton esters, where R represents an alkyl or aryl group.

Barton esters are used extensively for oxyl radical generation in synthesis,<sup>[85]</sup> as well as for kinetic investigations of radical activity.<sup>[86-88]</sup> This makes Barton esters attractive candidates as photolyses, as they possess well outlined radical chemistry.

The photosensitivity of *N*-hydroxypyridinethione has been recognized for 50+ years,<sup>[89,90]</sup> but its ability to generate  $\cdot\text{OH}$  radicals *via* a photoinduced process only became clear in the early 1990s.<sup>[78-80,91]</sup> Electron-spin resonance<sup>[91]</sup> and chemical trapping<sup>[80]</sup> experiments have shown that the formation of  $\cdot\text{OH}$  radicals from *N*-hydroxypyridinethione occurs upon UV-irradiation in organic solvents,<sup>[80,91]</sup> as well as in aqueous media.<sup>[78,79,92]</sup> Photoexcitation of thiocarbonyl group results in formation of an

excited state. From the excited state the compound undergoes homolytic cleavage of the N-O bond, resulting in a pyridylthiyl radical (PyS $\cdot$ ) and a  $\cdot$ OH radical, Scheme 2.

**Scheme 2.** Photoinduced homolytic cleavage of the N-O bond in *N*-hydroxypyridinethione.



The biological effect of  $\cdot$ OH radicals, particularly their DNA cleaving and oxidative activity, has been extensively studied and has been comprehensively reviewed.<sup>[42,53]</sup> DNA cleavage and oxidation by peroxy ( $\cdot$ OOR) radicals has also been established,<sup>[93-96]</sup> but relatively speaking only a small amount of work has been done with alkoxy radicals to determine their effect on DNA.<sup>[97,98]</sup> The genotoxicity of alkoxy radicals has been considered to the largest extent by Adam and co-workers<sup>[40,96,98,99]</sup> as well as Theodorakis and co-workers,<sup>[37,52,100]</sup> who investigated a number of photoinduced ( $\lambda = 350$  nm) alkoxy radicals generated from appropriate *N*-alkoxypyridinethiones for their ability and proficiency in cleaving DNA. These researchers found evidence to support the fact that not only  $\cdot$ OH radicals, but also a number alkoxy radicals cause significant oxidative damage to DNA.

The aforementioned researchers used gel electrophoresis to observe photoinduced DNA damage by monitoring single strand breaks (SSBs) in supercoiled DNA. DNA SSBs result in the conversion of supercoiled DNA (native conformation) to open-circular DNA (relaxed conformation). This induced conformational change allows for separation by gel electrophoresis (covered more thoroughly in section 2.1.4), which in turn allows for observation of the efficiency with which a radical causes oxidative damage to DNA. The ability and efficiency of alkoxy radicals to induce DNA SSBs was determined by presence and intensity of open-circular form compared to that of supercoiled in UV-illuminated pictures of gel electrophoresis experiments.

Adam and co-workers were able to produce gel images that clearly showed significant presence of open-circular DNA when solutions of supercoiled DNA (10 mg/L in 5.0 mM  $\text{KH}_2\text{PO}_4$  buffer, pH 7.2, 40% acetonitrile as cosolvent) were irradiated ( $\lambda = 350$  nm) for 25-60 min in the presence of a *N*-alkoxy pyridinethiones.<sup>[40]</sup> Control experiments<sup>[40]</sup> carried out using irradiation in the absence of the *N*-alkoxy pyridinethiones showed DNA only in the unaltered supercoiled form indicating strand cleavage had not taken place. These results clearly showed that SSBs in DNA are being induced by alkoxy radicals formed upon irradiation *N*-alkoxy pyridinethiones at 1PA wavelengths.

The results described above clearly demonstrate that *N*-alkoxy pyridinethiones are effective photonucleases when excited through 1PA ( $\lambda = 350$  nm). The interest of this thesis (thoroughly covered in the scope section, 2.5) is to investigate the ability of *N*-alkoxy pyridinethiones and other similar derivatives to produce DNA single strand cleavage through a 2PA event, using near IR-light ( $\lambda = 775$  nm). This would allow for the benefits of 2PA, i.e. use of longer wavelength light allowing for deeper penetration and

less toxicity when dealing with biological tissue, as well as better spatial control limiting peripheral tissue damage, to be applied to the study of radical effects on cell growth and viability in biological systems.

### *2.1.3 Free Radicals: Applications Photodynamic Therapy*

PDT has been recognized as an applicable and potentially highly effective method of therapy for hundreds of years.<sup>[101]</sup> First used in extensive clinical trials in the 1980s PDT has come to the leading edge of photomedicine and presents itself as an optimal candidate for future advancements in the photomedicine field.<sup>[102]</sup> PDT is a minimally invasive medical procedure that exploits the cytotoxic effects of light-activated compounds to achieve spatially selective tissue eradication. This procedure has been used in treating a range of cancerous diseases<sup>[103]</sup> and infections,<sup>[104]</sup> and recently in ophthalmology to treat age related macular degeneration (AMD).<sup>[105]</sup> Treatment with PDT involves application of a non-toxic photosensitizer that is preferentially taken up by the target cell/tissue. Optical excitation of the photosensitizer with appropriate wavelength generates a reactive oxygen species (ROS). Figure 12 displays the basic process of PDT. A photosensitizer or a photoreagent (e.g. R'OR) that prior to exposure to light is stable and has no toxic effects on the cell is introduced to the cell. Upon irradiation the reagent generates reactive oxygen species (ROS), such as hydroxyl or alkoxy radicals that then cause degradation of key cellular components, such as nucleic acids, proteins and lipids.<sup>[105]</sup> At sufficient levels degradation of these cellular components will induce cell death.



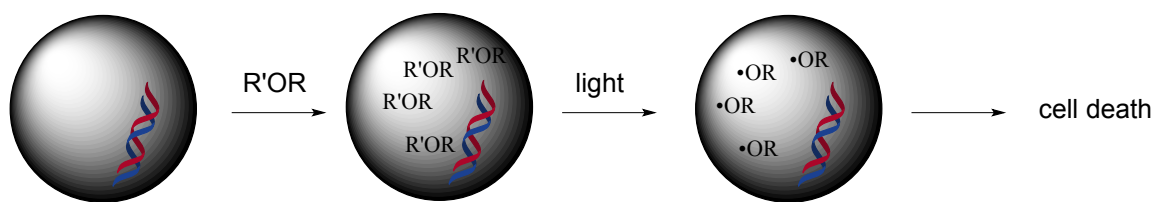


Figure 12. Illustration of the basic process of PDT.

Creation of short-lived ROS within biological tissue/cells creates localized cell death *via* irreversible damage to key cellular components such as DNA, proteins and lipids.<sup>[105]</sup> The life span of ROS within cells is very short,  $\sim 3 \mu\text{s}$  for singlet oxygen,<sup>[106]</sup> and  $\sim 4 \text{ ns}$  for oxygen radicals.<sup>[107]</sup> The diffusion distance and in turn the area of intracellular activity has been estimated at  $1000 \text{ \AA}$  for singlet-oxygen,<sup>[108-109]</sup> and  $90 \text{ \AA}$  for oxygen radicals.<sup>[107]</sup> Spectroscopic data collected from cells<sup>[109-112]</sup> indicates that ROS species are unable to diffuse through cellular membranes and into intercellular domains in which they were not produced. This is due to their limited life span as well as the high viscosity of the intracellular environment.<sup>[102]</sup> The limited diffusion capabilities of ROS species means that diffusion is only possible on an intracellular level, which implies that the first site of cell damage occurs at the point of ROS generation and damage will thus be contained to a single cell. With this knowledge of ROS diffusion it becomes obvious that photosensitizers must be accurately localized in a subcellular sense, as well be selectively accumulated and irradiated within targeted disease cells.

### 2.1.3.1 Free Radicals: Applications- Two-photon Excitation PDT (2PE-PDT)

Regardless of whether excitation of a photosensitive material used in PDT takes place by one-photon absorption or two-photon absorption, the general consensus is that both methods for excitation end up creating the same excited state.<sup>[113,114]</sup> Thus, the chemistry that occurs after excitation is the same for both 1PA and 2PA methods. The difference lies in the mode of excitation, and it is here where 2PA methods provide two clear advantages of 1PA. The first is the previously mentioned enhanced spatial control of the excitation volume (*vide supra*) that can be achieved with 2PA wavelengths, compared to 1PA wavelengths. This allows for the potential of highly spatially selective excitation of photosensitizers in tight region around the focal point of the irradiating laser beam.

Highly sensitive spatial control was demonstrated by Collins *et al.*<sup>[115]</sup> in a study where they presented a new family of photodynamic therapy drugs designed for efficient 2PA and used one of them to demonstrate selective closure of blood vessels through 2PE-PDT *in vivo*. They were able to demonstrate closure of individual blood vessels showing a highly selective nature that had not previously been shown with traditional one-photon excitation PDT (1PE-PDT). This result showed that 2PE-PDT could be performed with very minimal collateral damage to other tissue in the vicinity, and thus can alleviate the issues with selectivity and spatial control of 1PE-PDT.

The second advantage is that 2PE-PDT is able to penetrate deeper into biological tissue, as the irradiating beam will not be attenuated as strongly as a beam tuned for 1PE-PDT. This arises from less light scattering and tissue absorption experienced at 2PA wavelengths (*vide supra*). The ability of 2PE-PDT to penetrate more deeply into biological tissue makes excitation of photoreagents deeper within tissue possible. This is

especially significant when dealing with tissue that has an intact epidermal compartment; this kind of tissue is highly scattering and strongly hinders IPE-PDT.<sup>[116]</sup>

#### *2.1.4 Free Radicals: Observing DNA Damage via Gel Electrophoresis*

Gel electrophoresis is a method of separation that is used for the analysis of macromolecules, such as DNA, RNA, and proteins, as well as their fragments. It is a very commonly used technique in the fields of biochemistry and biology where it is used to separate mixed populations of DNA or RNA fragments based size, or more specifically length in base pairs (bp). This thesis only uses gel electrophoresis to analyze DNA and therefore RNA and protein electrophoresis will not be mentioned in this section but for interest can be found in this review,<sup>[117]</sup> which also includes more details on DNA electrophoresis.

DNA molecules are separated based primarily on their size, though the conformation of the DNA can also have a significant affect on separation, as seen the work of this thesis. Upon application of an electric field, DNA molecules (negatively charged due to the phosphate backbone) will migrate through the gel matrix toward the anode. Smaller DNA fragments will migrate a greater distance than larger ones as they more easily pass through the pores of the gel matrix; this phenomenon is known as sieving. Additionally, DNA molecules that are in the tightly wound, supercoiled conformation will migrate a greater distances than DNA molecules in a more relaxed open-circular conformation (result of strand cleavage). This is again due to greater ability of the DNA to sieve through the matrix pores when tightly wound as compared to when in a relaxed conformation. Agarose, the matrix used in this thesis, is composed of long

unbranched chains of uncharged carbohydrates without cross links giving a matrix with large pores allowing for the separation of larger macromolecules (DNA > 100 base pairs). The neutral charge and simple chemical complexity make this matrix ideal, as interactions with migrating molecules are not common.

An example of DNA separation based solely on DNA conformation can be found when working with plasmids. In their native conformation the plasmid DNA is supercoiled (twisted in on itself making a tightly knotted shape). After an induced strand break caused by an exogenous source, as performed in this thesis, the supercoiled DNA gets nicked and relaxes into a larger open-circular conformation. Figure 15 shows a hypothetical result for the separation caused between supercoiled and open-circular DNA after migration through a matrix has been completed. It should be noted that the DNA in both conformations are the same length in terms of number of base pairs, but have different effective sizes, making their separation using a gel electrophoresis possible. Once the electric field is applied for an appropriate amount of time to allow for separation, the gel can be viewed for analysis. DNA in either supercoiled or open-circular conformation will travel equal distance to other DNA molecules in the same conformation. This results in bands (darkened strips in Figure 15) appearing on the gel corresponding to the conformation of the DNA molecules present. These bands can be visualized by staining the gel with ethidium bromide, which when intercalated into DNA will fluoresce under UV light. The intensity of the band fluorescence can also be used to determine the relative concentration of DNA present in the varying conformations (thoroughly covered in section 3.1).

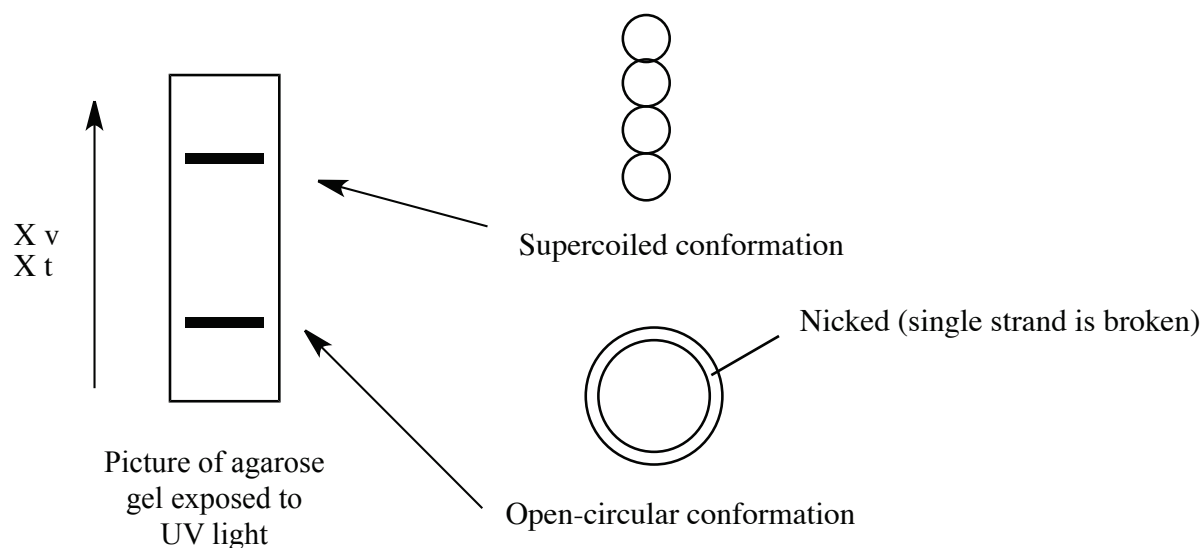


Figure 15. Hypothetical result for the separation of supercoiled and open-circular DNA after migration through an agarose matrix, and a UV illuminated picture of the gel has been acquired.  $X_v$  and  $X_t$  represent voltage of the applied electric field ( $v$ ) and the time ( $t$ ), which the electric field has been applied for. Darkened strips represent the fluorescent bands indicating the presence of DNA.

## 2.2 Scope of this Thesis

The general goal of this thesis is focused on demonstrating the utility of two-photon excitation in biological applications such as cleavage of DNA. In particular, the cleavage of DNA caused by the generation of oxygen-centered radicals formed upon two-photon excitation of *N*-oxypyridinethiones is explored. Figure 16 displays the structure of the pyridinethiones **1a** - **1f** investigated in this work.

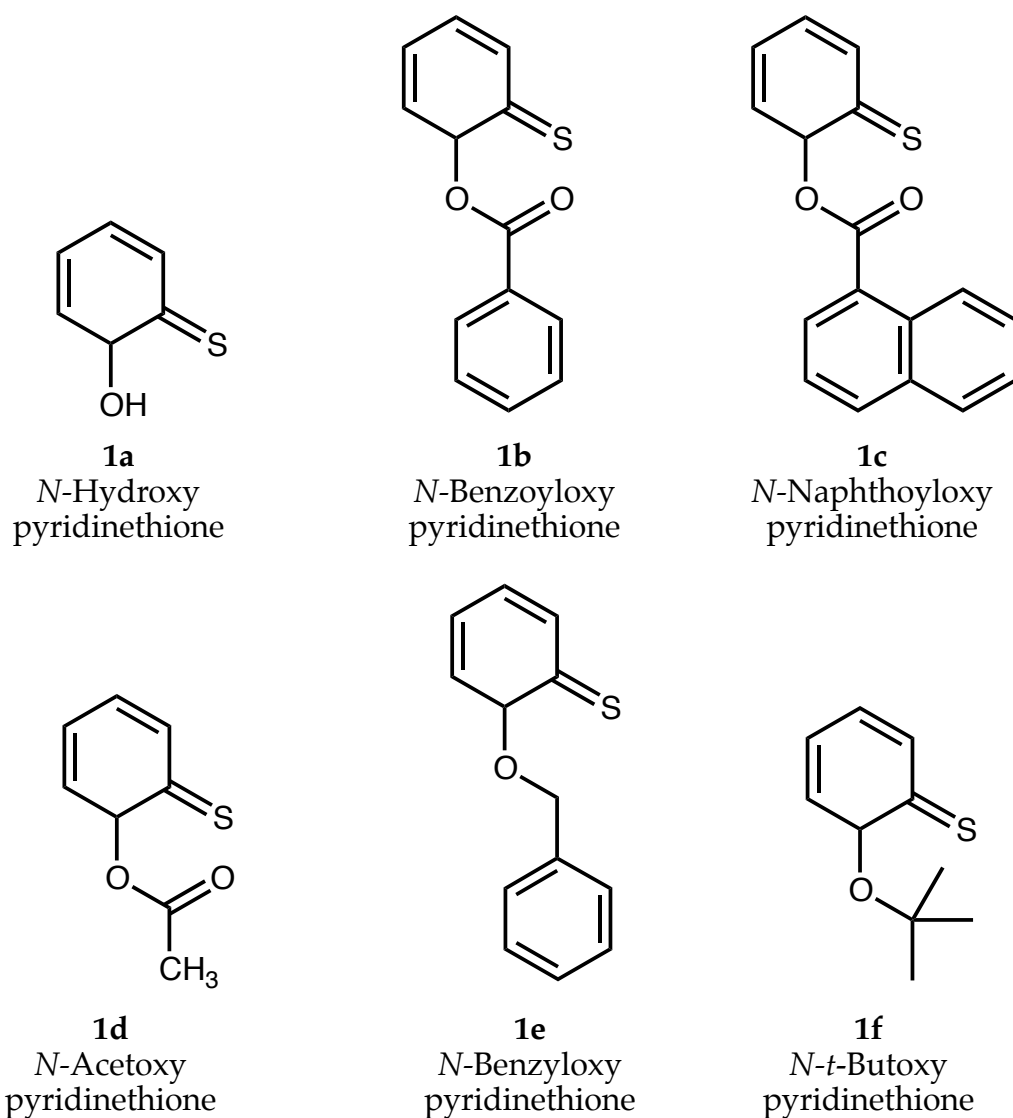


Figure 16. Structures *N*-oxypyridinethiones **1a** - **1f**.

The approach involves forming a series of oxygen-centered radicals in the presence of DNA *via* two-photon excitation of compounds **1a** - **1f** using a high intensity pulsed femtosecond laser and then determining the extent of DNA cleavage using gel electrophoresis. An attempt is made to observe the effect of structure on the efficiency of the two-photon induced cleavage of DNA.

## **CHAPTER 3 RESULTS AND DISCUSSION**

### *3.1 Observing and Quantifying DNA Strand Breaks*

It is necessary to first provide an explanation of how the results were obtained and interpreted to provide the reader with a better understanding of the data presented, particularly the conversion percentages referred to throughout this chapter. As described in the introduction, and as seen in works by several groups<sup>[36-38,40,69]</sup>, strand breaks in DNA can be monitored by gel electrophoresis. The experiments in this thesis employ this technique to observe and quantify the efficiency by which two-photon generated radicals induce SSBs in DNA. More efficient strand cleaving will lead to more conversion of DNA to the open-circular form from its native supercoiled conformation. Conformational changes are observed by separation provided through gel electrophoresis, by the same means outlined in the introduction. Quantification was done by looking at the fluorescence intensity of the open-circular band compared to that of the supercoiled band in pictures of gels that had been exposed to UV light. The intensity of bands on a gel directly relates to the concentration of DNA in the given band. This is based on the fact that ethidium bromide, the gel stain, fluoresces under UV light when intercalated with DNA. More DNA molecules will result in more binding sites for ethidium bromide, and in turn stronger fluorescence intensity will appear. With this knowledge, it can be estimated that the relative number of DNA molecules in a band is represented by the intensity of that band. By combining the open-circular band intensity with the supercoiled in the same lane (same sample) and subtracting the intensity of the background, one can obtain an intensity value that is representative of approximately 100% of the DNA in that sample. From here the percent converted to open-circular from supercoiled can easily be calculated by eq. 3:



$$\% \text{ open circular} = \frac{\text{intensity open circular} - \text{background}}{\text{summed intensity open circular and supercoiled} - \text{background}} \times 100\% \quad (3)$$

Percent conversions are not reported as an absolute measure but instead are meant to provide an approximate efficiency value so general conclusions may be drawn.

### *3.2 Experiments with pBR 322 DNA and N-Hydroxypyridinethione 1a*

A solution of *N*-hydroxypyridinethione **1a** (4.45 mM in acetonitrile) in the presence of buffered pBR 322 DNA ( $\leq 90$  % supercoiled, as tested by Sigma Aldrich, 0.5  $\mu\text{g}/\mu\text{L}$  10 mM Tris-HCl, pH 8.0, 1 mM EDTA) was irradiated for 3 h using 775 nm excitation from a femtosecond laser. The sample was then analyzed using gel electrophoresis and the results are presented in Figure 17, together with a second sample of pBR 322 DNA also irradiated for 3 h, but in the absence of **1a**.

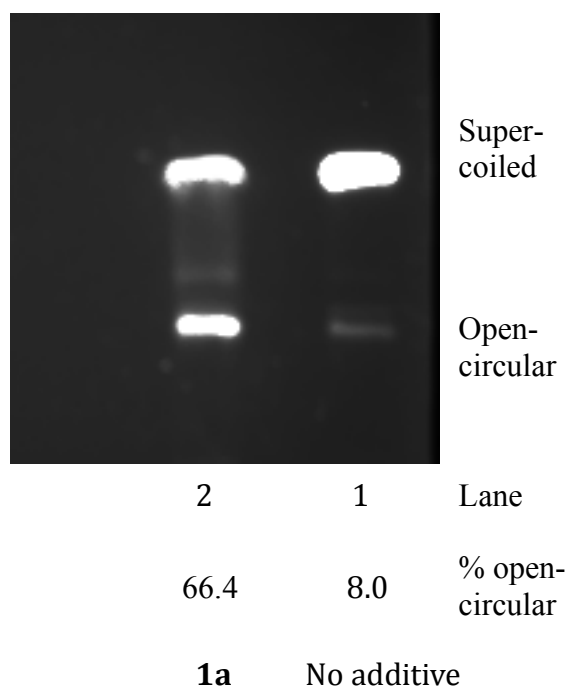


Figure 17. Gel electrophoresis analysis of pBR 322 DNA (0.5  $\mu\text{g}/\mu\text{L}$  in 10 mM Tris-HCl 1.0 mM EDTA buffer, pH 8.0): (lane 2) upon irradiation of *N*-hydroxypyridinethione **1a** (4.45 mM in acetonitrile) for 3 h by a femtosecond laser at 775 nm and (lane 1) upon irradiation for 3 h by a femtosecond laser at 775 nm in the absence of **1a**.

Figure 17 clearly shows that the DNA sample irradiated in the absence of **1a** (lane 1) contains only one intense band that corresponds to pBR 322 DNA in its unaltered supercoiled form. On the other hand, the sample irradiated in the presence of **1a** (lane 2) contains two intense bands, one corresponding to the unaltered supercoiled pBR 322 DNA and the other to the open-circular form of the pBR 322 DNA. The presence of the open-circular form clearly shows that two-photon excitation of **1a** leads to the single strand cleavage of DNA, similar to that already observed for one-photon excitation.<sup>[36-38,40,69,119]</sup> The intensity of the bands in both lanes 1 and 2 were measured as described in section 3.1, showing that the DNA sample in lane 2 was 66.4 % in the open-circular

form. This result shows that 3 h of femtosecond irradiation, 775 nm, of **1a** effectively causes single strand cleavage in DNA. The small amount of open-circular DNA in lane 2 suggests that the DNA is not sensitive to strand cleavage upon irradiation at 775 nm in the absence of the **1a**.

Irradiation at 775 nm of **1a** in the presence of pBR 322 DNA was repeated several times during the course of this work, giving values for the fraction converted to open-circular form ranging from 56.2 % to 66.4 %. An average value of  $60.3 \pm 3.0$  % was calculated from a sample size of 14 individual experiments using compound **1a** and pBR 322 DNA, and has a variance of 9.3.

A solution of **1a** (4.45 mM in acetonitrile) in the presence of pBR 322 DNA was left in the dark for 3 h. The sample was then analyzed using gel electrophoresis and the results are presented in Figure 18, together with a second sample of pBR 322 DNA also irradiated at 775 nm for 3 h in the absence of **1a**, and pBR 322 DNA irradiated at 775 nm for 3 h in the presence of **1a**.

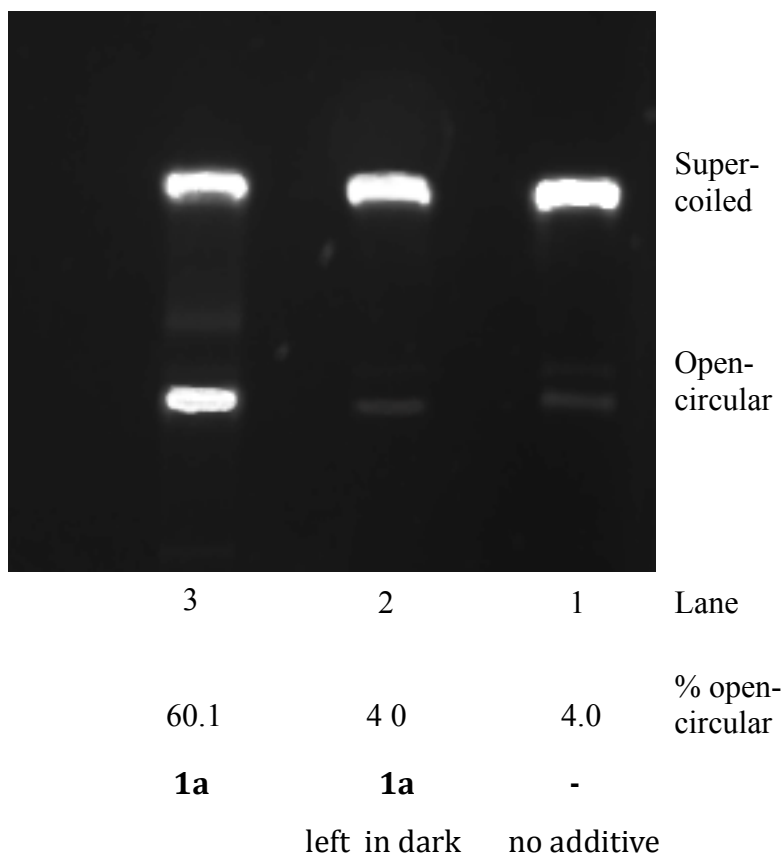


Figure 18. Gel electrophoresis analysis of pBR 322 DNA (0.5  $\mu\text{g}/\mu\text{L}$  in 10 mM Tris-HCl 1.0 mM EDTA buffer, pH 8.0): (lane 3) upon irradiation of *N*-hydroxypyridinethione **1a** (4.45 mM in acetonitrile) for 3 h by a femtosecond laser at 775 nm; (lane 2) with **1a** (4.45 mM in acetonitrile) in the dark for 3 h, and (lane 3) upon irradiation for 3 h by a femtosecond laser at 775 nm in the absence of **1a**.

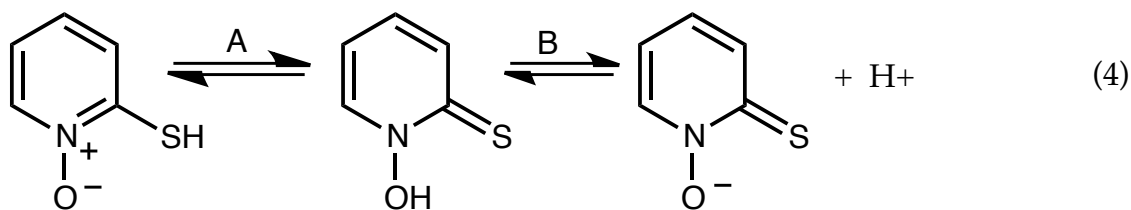
Again, Figure 18 shows that the DNA sample irradiated in the absence of **1a** (lane 1) contains only one intense band that corresponds to pBR 322 DNA in its unaltered supercoiled form. In addition, the results in Figure 18 show that the DNA sample in the presence of **1a** left in the dark for 3h (lane 2) also contains one band that corresponds to pBR 322 DNA in its unaltered supercoiled form. On the other hand, the sample irradiated

at 775 nm in the presence of **1a** (lane 3) contains two bands, one corresponding to the unaltered supercoiled form and the other to the open-circular form. The intensity of the bands in lanes 1, 2, and 3 were measured as described in section 3.1, showing that the DNA sample in lane 3 was 60.1 % in the open-circular form. This result again shows that 3 h of femtosecond irradiation with 775 nm of **1a** effectively causes single strand cleavage in DNA. The fact that the results in lanes 1 (irradiation in absence of **1a**) and 2 (no irradiation in the presence of **1a**) are the same indicates that the DNA is not sensitive to strand cleavage upon irradiation at 775 nm in the absence of the **1a**, and that the DNA is not sensitive to strand cleavage in the presence of **1a** unless the sample is irradiated.

The results presented in Figures 15 and 16 clearly show that DNA single strand cleavage is occurring upon two-photon photoexcitation of *N*-hydroxypyridinethione **1a** using 775 nm irradiation with femtosecond laser pulses. Presumably, upon excitation, **1a** undergoes N-O bond homolysis to give reactive products that subsequently cause DNA strand cleavage.

$\cdot\text{OH}$  radicals are generally assumed to be the oxidative species formed upon photoexcitation of **1a** that damage DNA and specifically induce single strand cleavage. However, it is worth noting that Redmond and co-workers<sup>[39,118]</sup> outline that in a cellular environment caution must be taken in the designation of **1a** as a “specific”  $\cdot\text{OH}$  radical generator. They acknowledge that excitation of **1a** does cause homolytic bond cleavage resulting in the formation of  $\text{PyS}\cdot$  radical and  $\cdot\text{OH}$  radical, as displayed in Scheme 2 (*vide supra*), but **1a** still cannot be designated a “specific”  $\cdot\text{OH}$  radical generator as other primary photoprocesses that produce potentially toxic species such as a triplet state, hydrated electrons and other radicals may occur.<sup>[118]</sup> Furthermore, it has been shown<sup>[55]</sup>

that in aqueous media photoexcitation of compound **1a** can be particularly slow and inefficient. This has been attributed to the tendency of **1a** to exist in equilibria of different forms, as shown in eq. 4<sup>[39, 55]</sup> These equilibria can be explained by the thione/thiol tautomerism (A) and acid/base equilibrium (B) ( $pK_a = 4.67$ ).<sup>[120]</sup> The equilibria in eq. 4 will decrease the concentration of thiocarbonyl containing species in biological media, thereby hampering the homolytic cleavage of the N-O bond and decreasing the concentration of  $\cdot\text{OH}$  radicals formed upon photoexcitation.



Despite the caveats outlined above, the results described above show that *N*-hydroxypyridinethione **1a** causes DNA cleavage upon two-photon induced excitation using femtosecond irradiation. In the subsequent sections, the efficiency by which **1a** causes two-photon induced cleavage is compared to that for other *N*-oxypyridinethiones **1b - f**.

### 3.3 Experiments with pBR 322 DNA and *N*-Benzoyloxypyridinethione **1b**

A solution of *N*-benzoyloxypyridinethione **1b** (4.45 mM in acetonitrile) in the presence of pBR 322 DNA (0.5  $\mu\text{g}/\mu\text{L}$  10 mM Tris-HCl, pH 8.0, 1 mM EDTA) was irradiated for 3 h using 775 nm excitation from a femtosecond laser. The sample was then analyzed using gel electrophoresis and the results are presented in Figure 19, together with a second sample of pBR 322 DNA also irradiated for 3 h, but in the absence of **1b**.

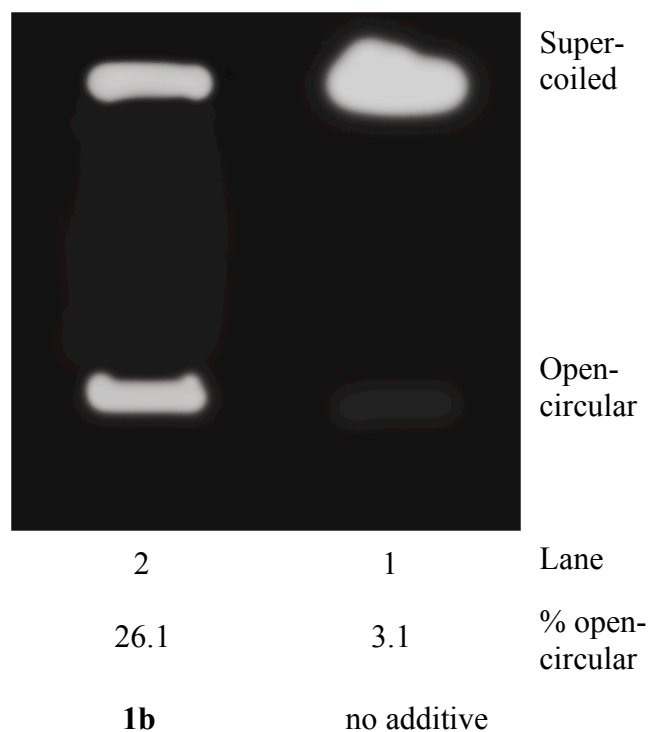


Figure 19. Gel electrophoresis analysis of pBR 322 DNA (0.5  $\mu\text{g}/\mu\text{L}$  in 10 mM Tris-HCl 1.0 mM EDTA buffer, pH 8.0): (lane 2) upon irradiation of **1b** (4.45 mM in acetonitrile) for 3 h by a femtosecond laser at 775 nm and (lane 1) upon irradiation for 3 h by a femtosecond laser at 775 nm in the absence of **1b**.

Figure 19 clearly shows that the DNA sample irradiated in the absence of **1b** (lane 1) only contains one intense band that corresponds to pBR 322 DNA in its unaltered supercoiled form. The sample irradiated in the presence of **1b** (lane 2) clearly contains two intense bands, one corresponding to the unaltered supercoiled pBR 322 DNA and the other to the open-circular form of the pBR 322 DNA. The presence of the open-circular form clearly shows that two-photon excitation of **1b** leads to the single strand cleavage of DNA, similar to that already observed for one-photon excitation of the same compound

under similar conditions.<sup>[36,38,54,100,119]</sup> The intensity of the bands in both lanes 1 and 2 were measured as described in section 3.1, showing that the DNA sample in lane 2 was 26.1 % in the open-circular form.

Irradiation at 775 nm of **1b** in the presence of pBR 322 DNA was repeated several times during the course of this work, giving values for the fraction converted to open-circular form ranging from 21.4. % to 26.1 %, giving an average value of  $23.9 \pm 1.7$  %. This average was calculated from a sample size of 7 individual experiments using *N*-benzoyloxypyridinethione **1b** and pBR 322 DNA, and has a variance of 3.2.

#### *3.4 Experiments with pBR322 DNA and N-Naphthoyloxypyridinethione 1c*

*N*-Naphthoyloxypyridinethione **1c** was investigated in order to provide additional insight into the cleaving efficiency of aroyloxy radicals. **1c** has not been previously reported as a radical precursor under any irradiation conditions, but it was hypothesized that it would follow the trend of **1b** and generate the correspond naphthoyloxy radical upon irradiation at 2PA wavelengths. A solution of **1c** (4.45 mM in acetonitrile) in the presence of buffered pBR 322 DNA (0.5  $\mu\text{g}/\mu\text{L}$  10 mM Tris-HCl, pH 8.0, 1 mM EDTA) was irradiated for 3 h using 775 nm excitation from a femtosecond laser. The sample was then analyzed using gel electrophoresis and the results are presented in Figure 20, together with a second sample of pBR 322 DNA irradiated for 3 h at 775 nm in the presence of **1a**, and an additional sample of pBR 322 DNA irradiated for 3 h at 775 nm in the absence of any additive compound.



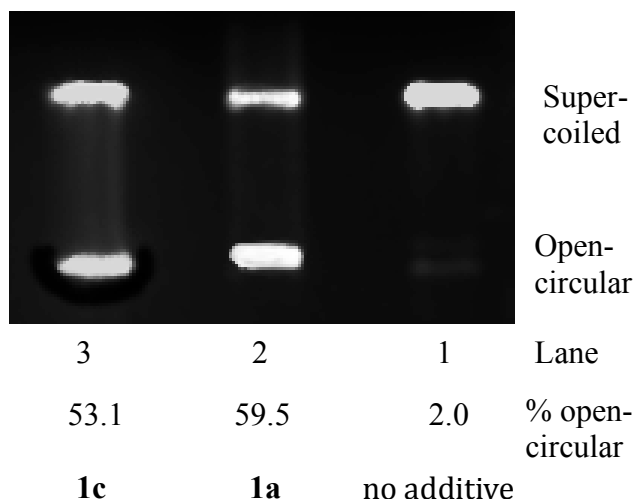


Figure 20. Gel electrophoresis analysis of pBR 322 DNA (0.5  $\mu\text{g}/\mu\text{L}$  in 10 mM Tris-HCl 1.0 mM EDTA buffer, pH 8.0): (lane 3) upon irradiation of *N*-naphthoyloxypyridine-thione **1c** (4.45 mM in acetonitrile) for 3 h by a femtosecond laser at 775 nm; (lane 2) upon irradiation of **1a** by a femtosecond laser at 775 nm for 3 h; and (lane 1) upon irradiation by a femtosecond laser at 775 nm for 3 h in the absence of any additive compound.

Figure 20 shows that the DNA sample irradiated in the absence of any additive compound (lane 1) only contains one band that corresponds to pBR 322 DNA in its unaltered supercoiled form. Alternatively, the sample irradiated in the presence of **1c** (lane 3) clearly contains two intense bands, one corresponding to the unaltered supercoiled pBR 322 DNA and the other to the open-circular form of the pBR 322 DNA, as does the sample irradiated in the presence of **1a**. The presence of the open-circular form clearly shows that two-photon excitation of **1c** leads to the single strand cleavage of DNA. The intensity of the bands in both lanes 1, 2, and 3 were measured as described in section 3.1, showing that the DNA sample with **1c** additive (lane 3) was 53.1 % in the open-circular form, as well the DNA sample with **1a** additive (lane 2) was 59.5 % in the

open-circular form. Thus, these data indicate that 3 h of femtosecond irradiation, 775 nm, of **1c** effectively causes single strand cleavage in DNA, as does **1a**.

Irradiation at 775 nm of **1c** in the presence of pBR 322 DNA was repeated a few times during the course of this work, giving values for the fraction converted to open-circular form ranging from 53.1 % to 61.4 %, giving an average value of  $57.0 \pm 4.1$  %. This average was calculated from a sample size of 3 individual experiments using *N*-naphthoyloxy pyridinethione **1c** and pBR 322 DNA, and has a variance of 16.9.

### *3.5 Experiments with pBR 322 DNA and N-Acetoxy pyridinethione 1d*

A solution of *N*-acetoxy pyridinethione **1d** (4.45 mM in acetonitrile) in the presence of buffered pBR 322 DNA (0.5  $\mu\text{g}/\mu\text{L}$  10 mM Tris-HCl, pH 8.0, 1 mM EDTA) was irradiated for 3 h using 775 nm excitation from a femtosecond laser. The sample was then analyzed using gel electrophoresis and the results are presented in Figure 21, together with a second sample of pBR 322 DNA also irradiated for 3 h, but in the absence of **1d**.

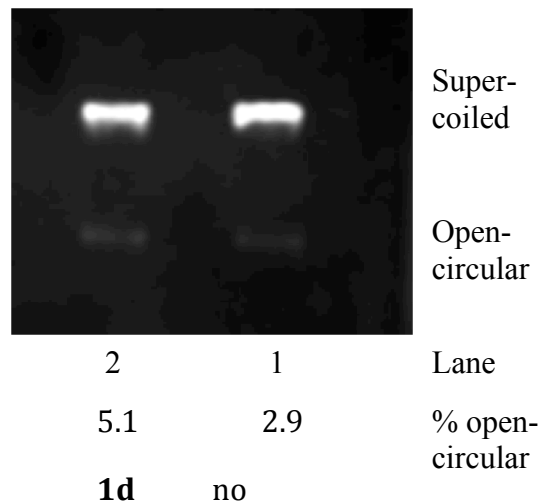


Figure 21. Gel electrophoresis analysis of pBR 322 DNA (0.5  $\mu\text{g}/\mu\text{L}$  in 10 mM Tris-HCl 1.0 mM EDTA buffer, pH 8.0): (lane 2) upon irradiation of *N*-acetoxy-pyridinethione **1d** (4.45 mM in acetonitrile) for 3 h by a femtosecond laser at 775 nm and (lane 1) upon irradiation by a femtosecond laser at 775 nm for 3 h in the absence of **1d**.

Figure 21 clearly shows that the DNA sample irradiated in the absence of any additive compound (lane 1) only contains one intense band that corresponds to pBR 322 DNA in its unaltered supercoiled form. The sample irradiated in the presence of **1d** (lane 2) also contains only one intense band, again corresponding to the unaltered supercoiled pBR 322 DNA. The absence of the open-circular form shows that two-photon excitation of **1d** does not lead to significant single strand cleavage of DNA.

Irradiation at 775 nm of **1d** in the presence of pBR 322 DNA was repeated twice during the course of this work, giving values for the fraction converted to open-circular form of 5.1 % and 3.9 %, for an average value of  $4.5 \pm 0.8$  %. This is similar to values obtained for control samples, that is samples of DNA not irradiated or samples irradiated

in the absence of an additive, which indicates that **1d** does not induce DNA strand cleavage upon two-photon irradiation.

### 3.6 Comparisons Between *O*-acyl Radical Generators **1b** - **d**

The results displayed in Figure 19 and Figure 20 show that aryloxy radical generators, *N*-benzoyloxypyridinethione **1b** and *N*-naphthoyloxypyridinethione **1c**, are effective two-photon photoreagents for DNA strand cleavage, causing  $23.9 \pm 1.7$  % and  $57.0 \pm 4.1$  % conversion of supercoiled DNA to open-circular form, respectively. Alternatively, *N*-acetoxypyridinethione **1d**, was found to produce no measurable strand cleavage beyond that of a DNA control,  $4.5 \pm 0.8$  %, as shown by the absence of a intense band due to the open-circular form of DNA in Figure 21. A range of factors must be considered in trying to explain the effect of structure on the ability of these substrates to cause DNA strand cleavage upon two-photon irradiation. One of these factors is the two-photon cross section of the compounds. Previous work by Schepp and colleagues<sup>[77]</sup> has shown that the two-photon cross section for the photodecomposition of *N*-naphthoyloxypyridinethione **1c** in acetonitrile is quite high,  $\delta = 0.21$  GM, compared to that for *N*-benzoyloxypyridinethione **1b** which has a two-photon cross section for photodecomposition of 0.062 GM and *N*-acetoxypyridinethione **1d** which has a slightly smaller two-photon cross section for photodecomposition of 0.052 GM. Two-photon cross sections for photodecomposition of compounds **1b** - **1d** are displayed in Table 1, along with observed DNA strand cleavage produced upon irradiation at 775 nm.

Table 1. Comparison of the two-photon cross sections for the decomposition of compounds **1b - d**, and their ability to cause DNA strand cleavage upon irradiation at 775 nm.

Compound	$\delta$ in acetonitrile (GM) <sup>[76]</sup>	% Strand cleavage after 3 h 775 nm laser irradiation
<i>N</i> -Benzoyloxy pyridinethione <b>1b</b>	0.062	23.9 ± 1.7
<i>N</i> -Naphthoyloxy pyridinethione <b>1c</b>	0.21	57.0 ± 4.1
<i>N</i> -Acetoxypyridinethione <b>1d</b>	0.052	4.5 ± 0.8

As can be seen from Table 1, compound **1b** has a two-photon cross section for decomposition that is about 3 times smaller than compound **1c**, which is similar to the 3 - fold decrease in the % strand cleavage. Thus, the efficiency of two-photon absorption does seem to play a major role in determining the effectiveness of these materials as substrates for two-photon induced DNA strand cleavage. On the other hand, the two photon cross section for **1d** is almost the same as that of **1b**, yet **1d** is much less efficient in its ability to initiate two-photon DNA strand cleavage. Thus, other factors must also play a role in determining the ability of these compounds to initiate DNA strand cleavage upon two-photon excitation.

It is known that O-acyl radicals can undergo decarboxylation to generate CO<sub>2</sub><sup>[54]</sup> and a carbon centered radical, with the rate of decarboxylation being dependent on the structure of the radical. Figure 22 displays the general structure of the resulting radicals formed upon homolytic cleavage of the N-O bond in compounds **1b - d**, as well as decarboxylation rate constants in acetonitrile,<sup>[121]</sup> and the general structure of the radicals that result from decarboxylation.

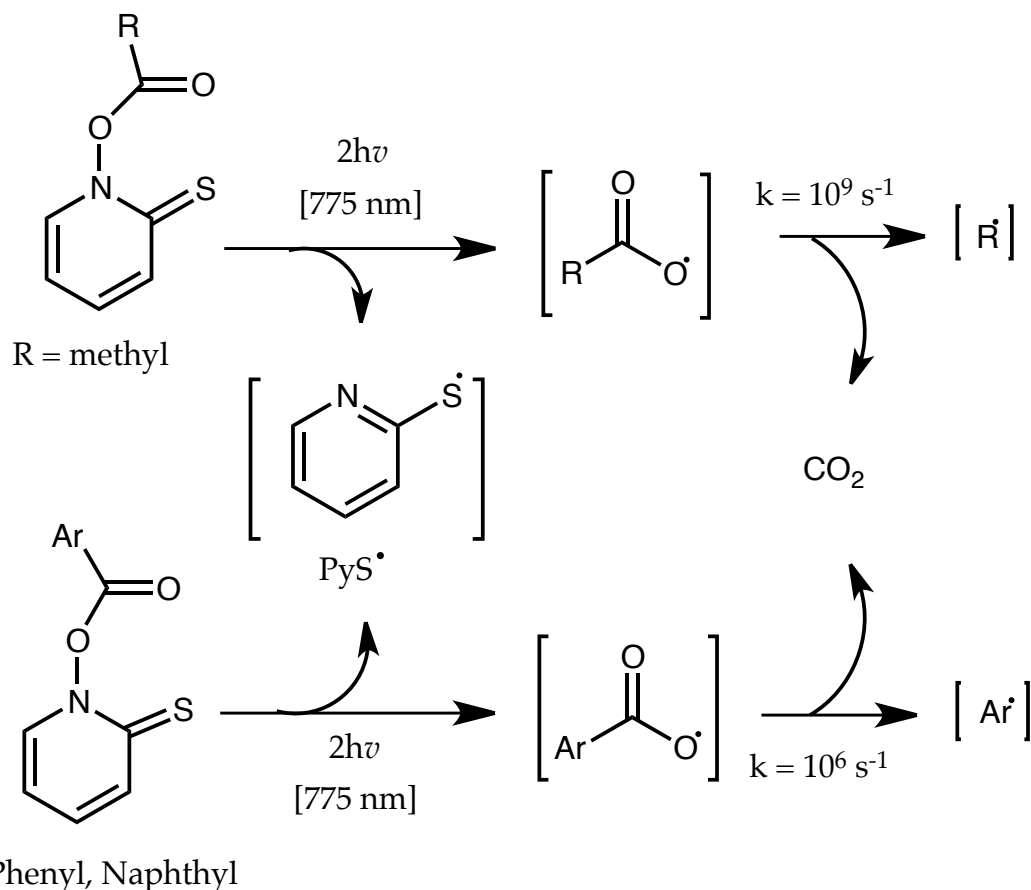


Figure 22. Formation and decarboxylation of carboxyl radicals. Rate constants<sup>[121]</sup> are for decarboxylation in acetonitrile. Ar = aryl or naphthyl group; R = alkyl group.

In general, oxygen-centered radicals are expected to be more reactive towards DNA, especially *via* hydrogen abstraction reactions, than carbon centered radicals. Thus, due on the rapid decarboxylation of the acyloxy radical,<sup>[121]</sup> the radicals produced from compound **1d** will not be as reactive toward DNA as compared to the aryloxy radicals that only reluctantly undergo decarboxylation. In other words, compound **1d** is not efficient in producing DNA strand cleavage upon two-photon excitation due its

photoproduct radical not being an effective agent for reaction with DNA. Alternatively, aryloxy radicals, which have a much slower decarboxylation rate ( $k = 10^6 \text{ s}^{-1}$ )<sup>[121]</sup> in acetonitrile, are able to participate in subsequent reactions with DNA, causing DNA strand cleavage before decarboxylation occurs.

It is worth noting that the discussion above presumes that the PyS· radical likely has negligible DNA cleaving effects. This is a reasonable presumption, since sulfur-centered radicals are not very reactive and the PyS· radical would likely dimerize to give PySSyP more rapidly than it would react with DNA.<sup>[118]</sup>

Another factor that must be taken into account is the ability of the **1b** and **1c** to coordinate with the DNA duplex prior to irradiation. Thus, both the benzyl and the naphthyl groups might, in principle, interact with the DNA duplex *via* intercalation, which occurs when a ligand of an acceptable size and chemical nature fits itself in between the base pairs of DNA.<sup>[143]</sup> Characteristics in compounds that have been reported to undergo DNA intercalation include being polycyclic, aromatic and planar.<sup>[122]</sup> A naphthalene group is more characteristic of an efficient DNA intercalator than is a phenyl or methyl group.<sup>[122]</sup> Thus, it is suggested that **1c** undergoes the greatest amount of intercalation with the duplex DNA prior to radical formation. Subsequent radical formation, upon irradiation, will occur in a position significantly more accessible to the DNA backbone, increasing the DNA cleaving efficiency. The absence or decrease of a prior interaction between compounds **1b** and **1d** with the DNA duplex may also play a role in the lesser and ability of these compounds to act as effective two-photon initiators of DNA cleavage as described above.

### 3.7 Experiments with pBR 322 DNA and *N*-Benzyloxypyridinethione **1e**

A solution of *N*-benzyloxypyridinethione **1e** (4.45 mM in acetonitrile) in the presence of buffered pBR 322 DNA (0.5  $\mu\text{g}/\mu\text{L}$  10 mM Tris-HCl, pH 8.0, 1 mM EDTA) was irradiated for 3 h using 775 nm excitation from a femtosecond laser. The sample was then analyzed using gel electrophoresis and the results are presented in Figure 23, together with a second sample of pBR 322 DNA also irradiated for 3 h, but in the absence of **1e**.

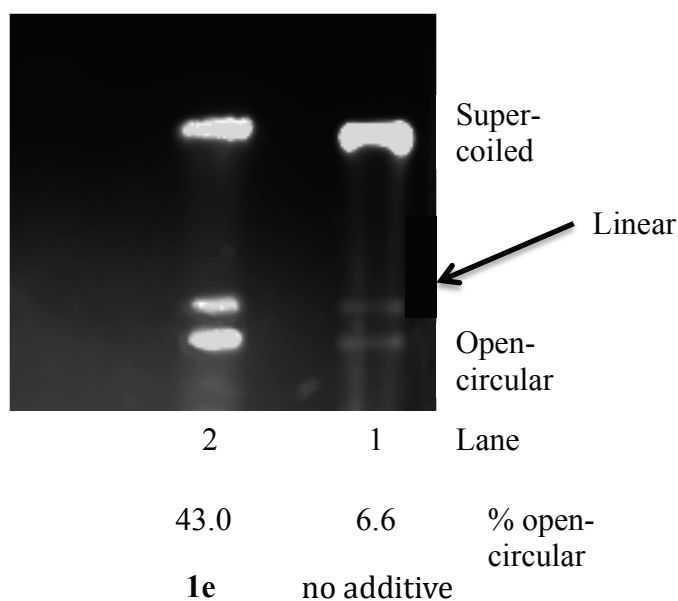


Figure 23. Gel electrophoresis analysis of pBR 322 DNA (0.5  $\mu\text{g}/\mu\text{L}$  in 10 mM Tris-HCl 1.0 mM EDTA buffer, pH 8.0): (lane 2) upon irradiation of *N*-benzyloxypyridinethione **1e** (4.45 mM in acetonitrile) for 3 h by a femtosecond laser at 775 nm and (lane 1) upon irradiation by a femtosecond laser at 775 nm for 3 h in the absence of **1e**.



Figure 23 shows that the DNA sample irradiated in the absence of **1e** (lane 1) only contains one intense band that corresponds to pBR 322 DNA in its unaltered supercoiled form. The sample irradiated in the presence of **1e** (lane 2) clearly contains three intense bands, one corresponding to unaltered supercoiled form, one to the open-circular form and one to the linear form of pBR 322 DNA, as indicated in Figure 23. The presence of the open-circular and linear DNA forms shows that two-photon excitation of **1e** leads to the single strand cleavage of DNA, and in this case double strand cleavage of DNA as well. The linear form of DNA observed in this experiment migrated a distance slightly further than open-circular form. Gel electrophoresis in this experiment was run for an additional 2 h at a lower voltage, 35 V, in an attempt to achieve greater separation and more resolution. This is the only experiment in which these varied electrophoresis-operating conditions were used. DNA converted to the linear conformation was included in the conversion percentage to open-circular form, as it signals that DNA cleavage has taken place.

The linear DNA conformation represents a double strand break in the DNA duplex. A double strand break will result in the plasmid no longer being continuous giving it a linear conformation. The increased run time and lower voltage of electrophoresis would result in greater separation between varying conformations, and this in turn could result in the visualization of both linear and open-circular forms of DNA. For the purpose of this work the intensity of linear form can be included in open-circular intensity, as its presence also signals that DNA strand cleavage is taking place.

A deeper investigation into why double strand cleavage was taking place in this case was not carried out, since the main goal of this work was to determine if these

substrates are good two-photon reagents for DNA strand cleavage in general. However, the fact that double strand cleavage is taking place may have importance for future work since double strand breaks are a particularly severe DNA lesion that can lead genomic rearrangement.<sup>[123]</sup>

Irradiation at 775 nm of **1e** (4.45 mM in acetonitrile) in the presence of pBR 322 DNA was repeated several times during the course of this work, giving values for the fraction converted to open-circular form ranging from 36.3 % to 43.0 %, giving an average value of  $39.8 \pm 2.6$  %. This average was calculated from a sample size of 5 individual experiments using *N*-benzyloxypyridinethione **1e** and pBR 322 DNA, and has a variance of 6.9.

Another experiment was also carried out with compounds *N*-benzyloxypyridinethione **1e** and *N*-benzoyloxypyridinethione **1b** to compare the efficiency of two-photon induced strand cleavage for the two substrates. *N*-Hydroxypyridinethione **1a** was also run in this experiment for efficiency comparison with  $\cdot\text{OH}$  radical. Solutions of compounds **1a**, **1b** and **1e** were all prepared to a concentration of 4.45 mM in acetonitrile. The solutions of **1a**, **1b** and **1e** were irradiated at 775 nm using a femtosecond laser in the presence of pBR 322 DNA (0.5  $\mu\text{g}/\mu\text{L}$  in 10 mM Tris-HCl 1.0 mM EDTA buffer, pH 8.0), as was pBR 322 DNA with no additive compound, the results for this experiment is displayed in Figure 24.

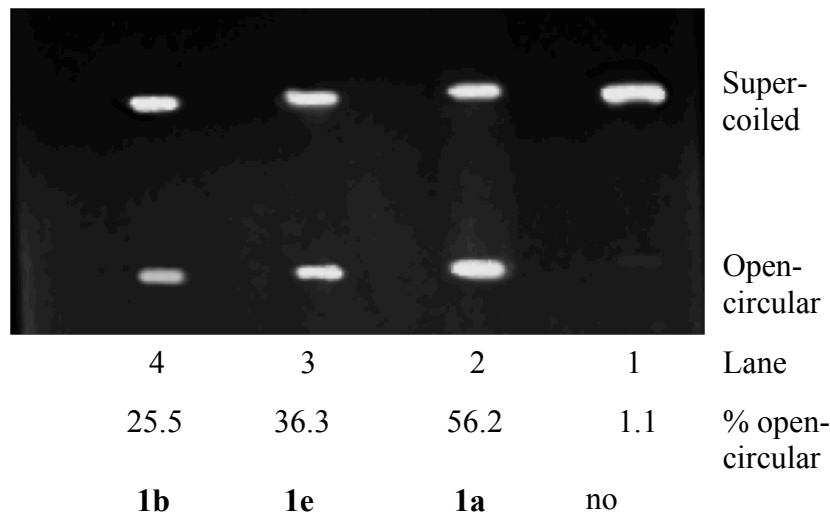


Figure 24. Gel electrophoresis analysis of pBR 322 DNA (0.5  $\mu\text{g}/\mu\text{L}$  in 10 mM Tris-HCl 1.0 mM EDTA buffer, pH 8.0): (lane 4) upon irradiation of *N*-benzoyloxypyridinethione **1b** (4.45 mM in acetonitrile) for 3 h by a femtosecond laser at 775 nm; (lane 3) upon irradiation of *N*-benzoyloxypyridinethione **1e** by a femtosecond laser at 775 nm for 3 h; (lane 2) upon irradiation of *N*-hydroxypyridinethione **1a**; and (lane 1) upon irradiation by a femtosecond laser at 775 nm for 3 h in the absence of any additive compound.

Figure 24 clearly shows that the DNA samples irradiated in the presence of all three pyridinethione additives **1a**, **1e**, and **1b**, lane 2, 3 and 4 respectively clearly contain two intense bands, one corresponding to the unaltered supercoiled pBR 322 DNA and the other to the open-circular form of the pBR 322 DNA. The presence of the open-circular form indicates that two-photon excitation of compound **1b**, **1e** and **1a** leads to the single strand cleavage of DNA. The intensity of the bands in all lanes was measured as described in section 3.1. Compound **1e**, a benzyloxyl radical generator, displayed more efficient strand cleaving capabilities (36.3 %) than compound **1b** (25.5 %), a benzoyloxyl radical generator. Presumably, one reason for the lesser ability of the benzoyloxyl radical to produce strand cleavage is that its acyl group provides stability to the radical through

resonance, while the methylene bridge in the benzyloxyl radical will provide significantly less stability to the radical. The less stable radical is expected to be the more reactive radical, which is consistent with the data shown in Figure 24.

### *3.8 Experiments with pBR 322 DNA and N-t-Butoxypyridinethione 1f*

A solution of *N-t*-butoxypyridinethione **1f** (4.45 mM in acetonitrile) in the presence of buffered pBR 322 DNA (0.5 µg/µL 10 mM Tris-HCl, pH 8.0, 1 mM EDTA) was irradiated for 3 h using 775 nm excitation from a femtosecond laser. Solutions of *N*-hydroxypyridinethione **1a**, *N*-benzoyloxypyridinethione **1b** and *N*-benzyloxypyridinethione **1e** (4.45 mM in acetonitrile) were also irradiated at 775 nm by a femtosecond laser for 3 h in the presence of pBR 322 DNA, as was pBR 322 DNA not in the presence of any additive. Figure 25 displays the results of this experiment.

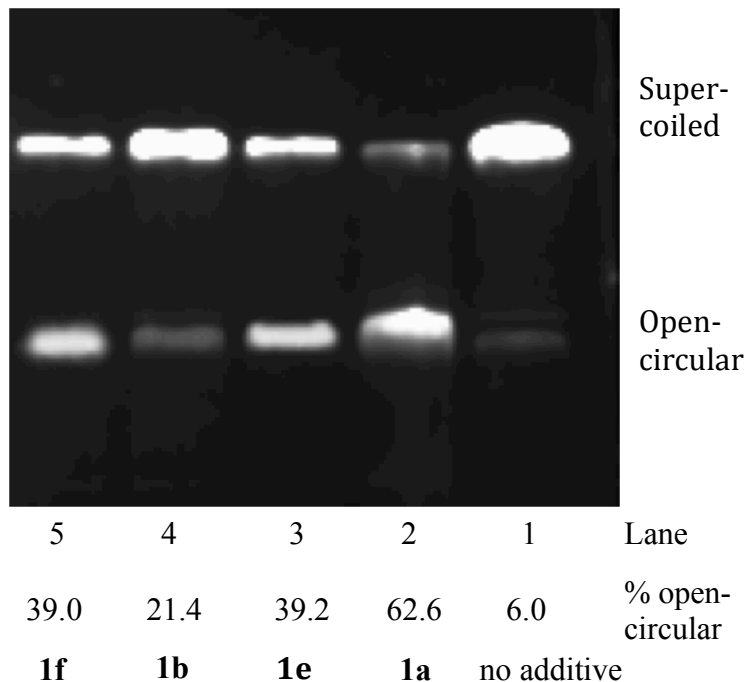


Figure 25. Gel electrophoresis analysis of pBR 322 DNA (0.5  $\mu\text{g}/\mu\text{L}$  in 10 mM Tris-HCl 1.0 mM EDTA buffer, pH 8.0): (lane 5) upon irradiation of *N-t*-butoxypyridinethione **1f** (4.45 mM in acetonitrile) for 3 h by a femtosecond laser at 775 nm; (lane 4) upon irradiation of *N*-benzoyloxypyridinethione **1b** by a femtosecond laser at 775 nm for 3 h; (lane 3) upon irradiation of *N*-benzoyloxypyridinethione **1e**; (lane 2) upon irradiation of *N*-hydroxypyridinethione **1a**; and (lane 1) upon irradiation by a femtosecond laser at 775 nm for 3 h in the absence of any additive compound.

Figure 25 shows that the DNA sample irradiated in the presence of **1f** (lane 2) contains two intense bands, one corresponding to the unaltered supercoiled pBR 322 DNA and the other to the open-circular form of the pBR 322 DNA. The presence of the open-circular form clearly shows that two-photon excitation of **1f** leads to the single strand cleavage of DNA. The intensity of the bands in all lanes were measured, showing that the DNA sample in lane 5, treated with **1f**, was 39.0 % in the open-circular form.

This result clearly shows that 3 h of femtosecond irradiation at 775 nm of *N-t*-butoxypyridinethione **1f** effectively causes single strand cleavage in DNA.

Irradiation at 775 nm of **1f** (4.45 mM in acetonitrile) in the presence of pBR 322 DNA was repeated two times during the course of this work, giving values for the fraction converted to open-circular form ranging from 37.3 % to 40.3 %, giving an average value of  $38.9 \pm 1.5$  %. This average was calculated from a sample size of 3 individual experiments using **1f** and pBR 322 DNA, and has a variance of 2.3.

Experiments done with *N*-benzyloxypyridinethione **1e** and *N-t*-butoxypyridinethione **1f** showed that the DNA cleavage ability of *t*-butoxy radicals **1f** ( $38.9 \pm 1.5$  % single strand cleavage) is very similar to that of a benzyloxyl radicals **1e** ( $39.8 \pm 2.6$  % single strand cleavage). This can be reasoned again by looking at the stability of the radicals generated upon photoexcitation. Neither the *t*-butyl group nor the methylene linked phenyl group will provide any significant stability to the radical center, and these two substrates would be expect to have similar reactivity. As well, these two compounds presumably have similar two-photon cross sections for decomposition, which would also lead to similar abilities to induce two-photon DNA cleavage. **1f** was thought to be more efficient than *N*-benzoyloxypyridinethione **1b** for the same reasoning as **1e**, radical stability. The acyl group in **1b** will provide more stability to the radical center than the *t*-butyl group in **1f**; this could result in the lesser cleavage ability observed for **1b**.

### 3.9 Comparisons between Radical Generators **1a** - **1f**

Conversion percentages from all experiments are tabulated in Table 2. Two-photon cross sections measured previously<sup>[77]</sup> for the two-photon induced decomposition

of the pyridinethiones are included in table 2. Additionally, a value for the % open-circular DNA form found in all experiments using pBR 322 DNA irradiated without a pyridinethione additive is given. This value,  $5.1 \pm 2.9$  %, falls within the expected range of open-circular conformation in unaltered pBR 322 DNA as reported by Sigma Aldrich to be tested at 10 % or less.

Table 2. Average conversion percentages to open-circular conformation upon irradiation at 775 nm for 3 h.

	% Strand cleavage after 3 hr 775 nm laser irradiation	$\delta$ in acetonitrile (GM) <sup>[77]</sup>
DNA (no additive)	$5.1 \pm 2.9$	----
<i>N</i> -Hydroxypyridinethione <b>1a</b>	$60.3 \pm 3.0$	0.018
<i>N</i> -Benzoyloxypryridinethione <b>1b</b>	$23.9 \pm 1.7$	0.062
<i>N</i> -Naphthoyloxypryridinethione <b>1c</b>	$57.0 \pm 4.1$	0.21
<i>N</i> -Acetoxypyridinethione <b>1d</b>	$4.5 \pm 0.8$	0.052
<i>N</i> -Benzyloxypryridinethione <b>1e</b>	$39.8 \pm 2.6$	0.037
<i>N</i> - <i>t</i> -Butoxypryridinethinoe <b>1f</b>	$38.9 \pm 1.5$	not measured

DNA cleaving efficiency was found to vary based on the structure of the group attached to the oxygen of the *N*-oxypryridinethiones **1a** - **1f**. It was found that the parent *N*-hydroxypyridinethione **1a** is the most effective strand cleaver under the uniform experimental conditions used throughout this work. Given that the two-photon cross section for decomposition of *N*-hydroxypyridinethione,  $\delta = 0.018$  GM, is the smallest of those measured in table 2 and that **1a** will not undergo any significant intercalation with

the DNA duplex prior to irradiation, the most likely reason for why **1a** is such an efficient two-photon agent for DNA cleavage is the extreme reactivity of the  $\cdot\text{OH}$  radical with the DNA duplex. *N*-Naphthoyloxy pyridinethione **1c** was also found to be a very efficient DNA strand cleaver. This can be attributed to having the highest reported two-photon cross section for decomposition,  $\delta = 0.21$  GM, and/or being an efficient DNA intercalator. Furthermore, the naphthoyloxy radical is not expected to undergo decarboxylation, so it is likely to be a reactive oxygen centered radical that also contributes to the ability of **1c** to be an effective agent for two-photon cleavage of DNA.

Despite the fact that the benzoyloxy radical generated from **1b** likely has a similar reactivity to the naphthoyloxy radical generated from **1c**, *N*-benzoyloxy pyridinethione **1b** was a significantly poorer substrate for two-photon induced cleavage than **1c**. Again, **1b** presumably does not intercalate as efficiently with DNA as **1c**, and the two-photon induced decomposition of **1b**,  $\delta = 0.092$  GM, is less than one-third that for **1c**,  $\delta = 0.21$  GM. These latter two factors presumably contribute to the overall decreased efficiency of **1b** as a substrate for two-photon induced cleavage.

The least efficient substrate for inducing two-photon DNA strand cleavage was *N*-acetoxypyridinethione **1d**, even though its two-photon cross section for decomposition was reasonably high at  $\delta = 0.051$  GM. In this case, the poor efficiency is likely due to the fact that the acetoxy radical generated from **1d** rapidly undergoes decarboxylation to give a less reactive carbon centered radical. Also, **1d** would not likely have an enhanced intercalation with DNA like other substrates such as **1c**.



3.10 Time Dependent Efficiency Experiment with pBR 322 DNA and *N*-Hydroxypyridinethione **1a**

*N*-Hydroxypyridinethione **1a** was further investigated in its ability to cleave pBR 322 DNA with an experiment designed to study the dependence of DNA strand breaks *via* two-photon excitation as a function of irradiation time. Femtosecond irradiation at 775 nm of a solution of **1a** (4.45 mM in acetonitrile) in the presence of buffered pBR 322 DNA (0.5  $\mu\text{g}/\mu\text{L}$  10 mM Tris-HCl, pH 8.0, 1 mM EDTA) was done for times of 0, 30, 60, 90, 120 and 180 min, the results of this experiment are displayed in Figure 26.

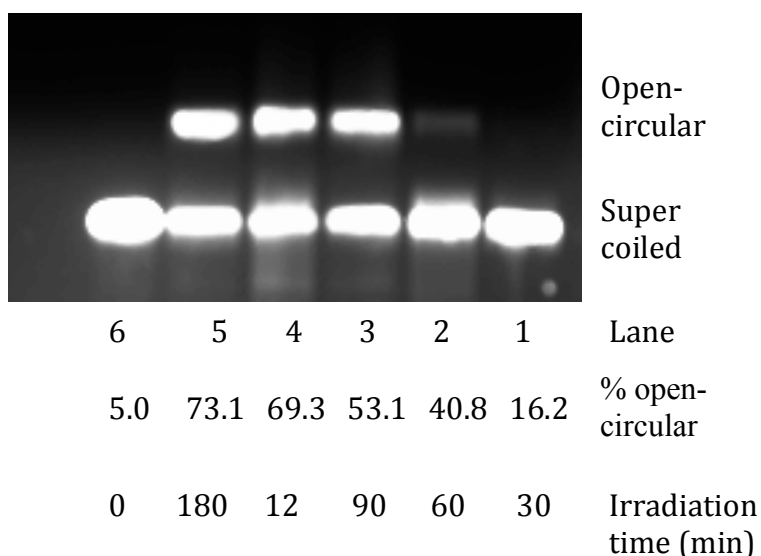


Figure 26. Gel electrophoresis analysis of strand breaks generated in pBR 322 DNA (0.5  $\mu\text{g}/\mu\text{L}$  10 mM Tris-HCl, pH 8.0, 1 mM EDTA) upon femtosecond irradiation of *N*-hydroxypyridinethione **1a** for 30, 60, 90, 120 and 180 min at 775 nm corresponding to lanes 1 – 5, respectively. pBR 322 DNA (0.5  $\mu\text{g}/\mu\text{L}$  10 mM Tris-HCl, pH 8.0, 1 mM EDTA) with **1a** additive (4.45 mM in acetonitrile) not exposed to irradiation is shown in lane 6.

Figure 27 displays the results from Figure 26 graphically in a scatter plot of fraction of supercoiled DNA versus time. As described in Chapter 4, the data shown in Figure 27 can be treated according to eq. 5 in order to determine the two-photon cross section,  $\delta$ , for DNA strand cleavage using 775 nm femtosecond irradiation of *N*-hydroxypyridinethione **1a**.

$$\frac{C_t}{C_o} = e^{-\delta \nu I_{\text{eff}} t} \quad (5)$$

In this equation,  $\nu$  is the pulse frequency of 1000 Hz,  $I_{\text{eff}}$  is the laser light flux (and is described in detail in chapter 4), and  $t$  is the irradiation time. Eq. 5 indicates that non-linear least squares fitting of the fraction supercoiled DNA remaining after various irradiation times will give the desired parameter  $\delta$ , which is the two-photon cross section for DNA strand cleavage using **1a**.

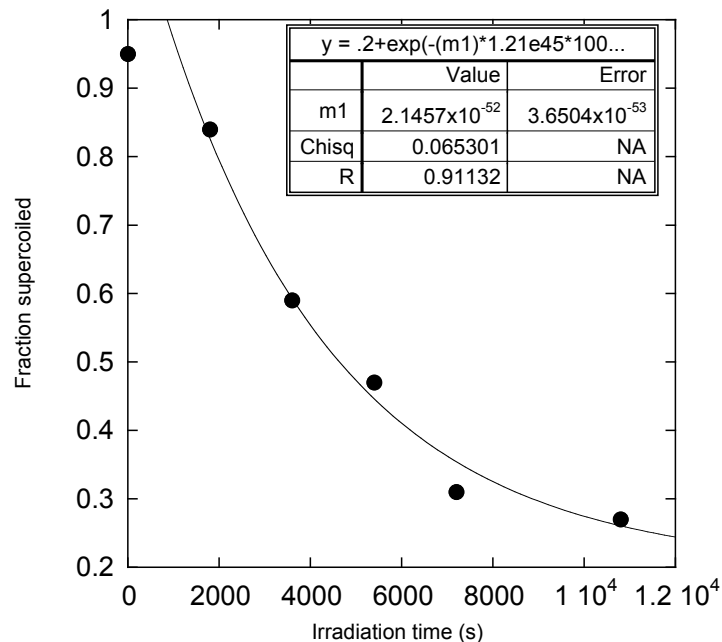


Figure 27. Results of time-dependent irradiation study using *N*-hydroxypyridinethione **1a** (4.45 mM in acetonitrile) and buffered pBR 322 DNA (0.5  $\mu\text{g}/\mu\text{L}$  10 mM Tris-HCl, pH 8.0, 1 mM EDTA). Results are displayed graphically in a fraction of supercoiled DNA versus irradiation time plot. Line of best fit added from non-linear least squares regression.

In this case, a value of  $\delta = 0.022$  GM was measured. This value is remarkably similar to a two-photon cross section of  $\delta = 0.018$  GM for decomposition of **1a** in acetonitrile solution using 775 nm light measured previously by Schepp and colleagues.<sup>[77]</sup> The similarity of these two values is consistent with the notion with that the radical formed by two-photon induced decomposition of **1a** is responsible for the observed DNA strand cleavage.

To our knowledge, no other measurements of two-photon cross sections for two-photon induced DNA cleavage have been made, so comparisons of the value of  $\delta = 0.022$  GM with other values is not possible. However, it is worth mentioning that a cross

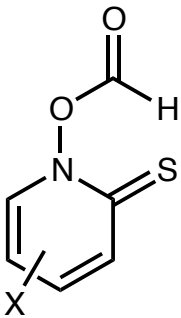
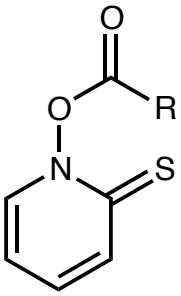
section of 0.022 GM is somewhat less than a cross section of 0.1 GM that is commonly thought to be the minimum value necessary for two-photon excitation to be useful in biological studies. Furthermore, while two-photon cross sections were not measured for the other *N*-alkoxy pyridinethiones used in the present work, the results presented earlier suggest that the parent *N*-hydroxypyridinethone **1a** was the most efficient material for DNA cleavage and the two-photon cross sections for compounds **1b - f** would likely be smaller.

## CHAPTER 4 TWO-PHOTON DECOMPOSITION OF *N*-ANTHRACENOYLOXYPYRIDINETHIONE

### 4.1 Introduction

Over the past few years, Schepp and colleagues have been investigating the effect of structure on the two-photon induced photoreactivity of relatively small organic chromophores, specifically the effect of structure on the two-photon photodecomposition of *N*-alkoxy-pyridinethiones. A summary of data obtained so far is shown in Table 3.

Table 3. Effect of structure on the two-photon cross section for the photodecomposition of *N*-alkoxy-pyridinethiones (Schepp, unpublished results).<sup>[77]</sup>

			
X	$\delta$ /GM	R	$\delta$ /GM
H	0.062	Ad	0.062
4-CN	0.026	PhCH <sub>2</sub>	0.13
4-CF <sub>3</sub>	0.042	Ph	0.051
3-CF <sub>3</sub>	0.023	Naph	0.21
4-C(O)O <i>i</i> Pr	0.042		
4-CH <sub>3</sub>	0.083		
4-OCH <sub>3</sub>	0.038		

These results show that electron donating or withdrawing substituents on the pyridinethione ring (Table 3, columns on the left) do not have a great effect on enhancing the two-photon cross section,  $\delta$ , compared to the parent H substituted compound ( $\delta = 0.062$  GM). Yet, a significant increase in the two-photon cross section is observed when the carboxylate moiety is changed from benzoyloxy to naphthoyloxy (Table 3, columns on the right). Thus, the data suggest that the two-photon cleavage of *N*-naphthoyloxy esters is more efficient than that for *N*-benzoyloxy esters.

This is a surprising result, since the main chromophore of these systems is the pyridinethione moiety, with the carboxylate fragment not expected to participate in the ability of the compound to undergo two-photon excitation. One possibility that was suggested previously (D. Halverson-Smith, Dalhousie Honours Project, 2011)<sup>[124]</sup> is that the aryl group of the carboxylate segment can orient itself so that it sits above the pyridinethione ring. In this orientation a charge transfer interaction can take place that may enhance the ability of the chromophore to undergo two-photon excitation.

Several ways have been suggested to test this hypothesis. One method is to make the carboxylate segment more floppy, thus allowing for the appropriate conformation to be more easily accessible. Alternatively, one could add electron-donating or withdrawing groups to the benzoyloxy and/or naphthoyloxy fragments to see if these influence the two-photon cross section. In addition, the size of the aromatic ring attached to the carboxylate segment can be increased, such as by using an anthracenoyloxy group. In this section, results obtained using the *N*-anthracenoyloxy pyridinethione (compound **1g**), are described. Figure 28 displays the structure of compound **1g**.

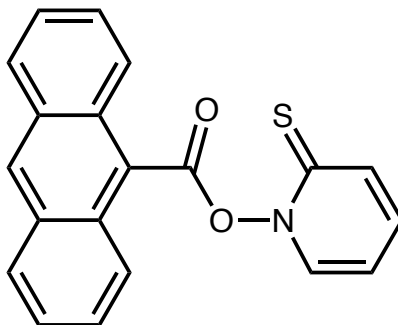


Figure 28. Structure of *N*-anthracenoyloxypyridinethione **1g**.

## 4.2 Results and Discussion.

### 4.2.1 Two-photon Cross Section: Mathematical Equations

As stated earlier, the main goal for this segment of my work was to measure the two-photon cross section,  $\delta$ , for the decomposition of *N*-anthracenoyloxypyridinethione **1g**. As described by Poloukhine *et al.*,<sup>[125]</sup> this can be achieved by measuring the fraction of substrate remaining ( $C_t/C_o$ ) after a specific time period of femtosecond laser irradiation using 775 nm light, as shown in eq. 5.

$$\frac{C_t}{C_o} = e^{-\delta \nu I_{eff} t_{corr}} \quad (5)$$

The fraction of substrate remaining can be readily measured from absorption spectra obtained before and after femtosecond laser irradiation, and these results are shown in the next section. The parameter  $\delta$  is the unknown two-photon cross section. The variable  $\nu$  in eq. 5 is the pulse frequency of 1000 Hz for the laser system used in this study. The time period of femtosecond laser irradiation is corrected to give  $t_{corrected}$ , accounting for the fact that only 9.2 % of the solution within the cuvette is being irradiated with the laser. In

other words, in these experiments, the total volume of the substrate solution used is 1.5 mL. However, the radius of the laser beam is only 0.21 cm. Since the path length is 1 cm and the laser radius is 0.21 cm, the laser only irradiates 0.14 mL of the 1.5 mL solution, as calculated using eq. 5.1.

$$\begin{aligned} \text{laser irradiation volume} &= \pi \times r^2 \times \text{pathlength} \\ &= \pi \times 0.21 \text{ cm}^2 \times 1 \text{ cm} = 0.14 \text{ mL} \end{aligned} \quad (5.1)$$

Thus, only 9.2 % of the solution (0.14 mL/1.5 mL) is irradiated, and this is accounted for by correcting the irradiation time by the same fraction. In other words, the time correction is based on the assumption that irradiating 9.2 % of a solution for 1000 s would be equivalent to irradiating the entire solution for 92 s.

The parameter  $I_{eff}$  in eq. 5 is the effective light intensity per laser pulse, and can be calculated using eq. 5.2.

$$I_{eff} = A^2 \int_{-t}^t e^{\frac{-t^2}{2C^2}} \quad (5.2)$$

In this equation, C is related the full width at half-maximum,  $w_{1/2}$ , of the laser pulse as shown in eq. 5.3. In these experiments,  $w_{1/2}$  was measured to be  $200 \pm 10$  fs, giving C a value of  $8.49 \times 10^{-14}$  s.

$$C = \frac{w_{1/2}}{2\sqrt{2\ln 2}} \quad (5.3)$$

The parameter A in eq. 5.2 is the light flux, and is calculated using eq. 5.4.

$$A = \frac{J / \text{pulse}}{\frac{hc}{\lambda} \pi r^2 \times C \sqrt{2\pi}} \quad (5.4)$$



Joules/pulse as determined by measuring the output from the laser with a power meter was 0.580 J,  $\lambda$  is excitation wavelength of 775 nm,  $r$  is the laser radius of 0.21 cm. Using these values,  $A$  is calculated to be  $7.67 \times 10^{28}$  photons  $\text{cm}^{-2} \text{s}^{-1}$ .

#### 4.2.2 Two-photon Cross Section: Experimental Results

Figure 29 shows the absorption spectrum of *N*-anthracenoyloxypyridinethione **1g** dissolved in acetonitrile prior to irradiation. The solution has a strong absorption at 370 nm that clearly extends beyond 400 nm into the visible region of the electromagnetic spectrum. This absorption spectrum is similar to that for other *N*-alkoxypyridinethiones measured by Schepp and colleagues,<sup>[77]</sup> although the weak shoulders near 350 nm and 380 nm are presumably due to the anthracenoyloxy group, which also has absorption in this region.

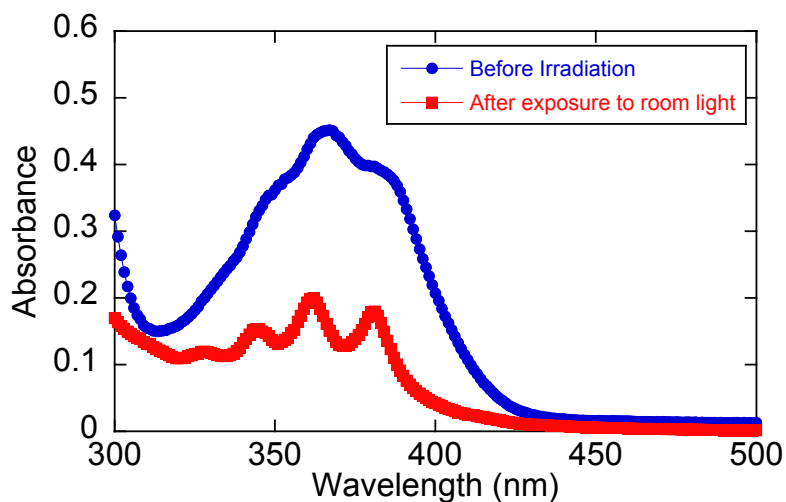
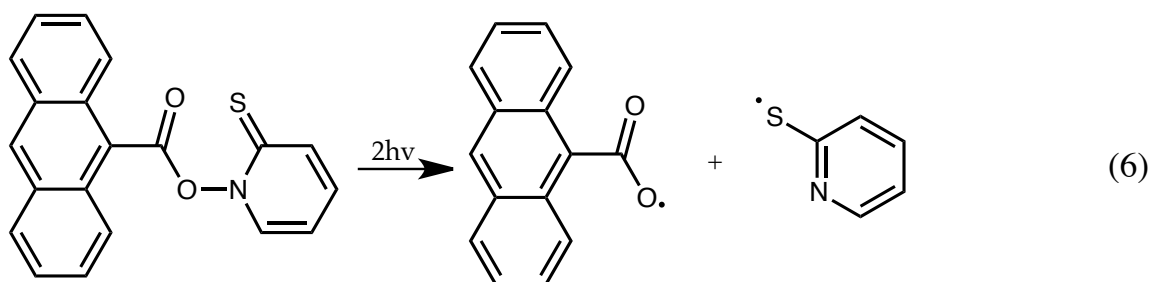


Figure 29. Absorption spectra of *N*-anthracenoyloxypyridinethione **1g** ( $10^{-5}$  M) in acetonitrile before and after exposure to room light for 1 min.

**1g** is very sensitive to room light, as shown by the fact that exposure to room light for one minute dramatically changes the spectrum to one that contains features expected for a simple anthracene derivative. Further exposure to room light caused no additional change, indicating that photodecomposition was complete after one min of exposure. Since the final spectrum is similar to that for a free anthracene derivative, the assumption is made that photodecomposition involved the conversion of **1g** to the PyS $\cdot$  radical and the anthracenoyloxyl radical, eq. 6, that then presumably undergoes other reaction(s) to give the anthracene derivative observed in the spectrum.



Having established that **1g** is sensitive to one-photon irradiation from room light, experiments were carried out to obtain the data required to for the two-photon cross section as shown above in eq. 5. This requires measuring the absorbance of the solution before femtosecond irradiation, and after femtosecond irradiation for various time periods. These data are shown below in Figure 30. In Figure 30, the first absorption spectrum is a solution of **1g** in acetonitrile prior to irradiation, and the next eight spectra, sub sequentially going down in absorbance, were obtained after femtosecond irradiation of the **1g** solution for 20 min intervals. The ninth spectrum, maximum absorbance at 0.3, was obtained after the solution of **1g** was irradiated at 775 nm for 6 h. And the final

spectrum, absorbance maximum at 0.2, was obtained after exposure of the **1g** solution to room light for 5 min, representing complete decomposition the sample, so that an absorbance at  $t_{inf}$  could be obtained.

The data in Figure 30 clearly show that **1g** in acetonitrile is sensitive to two-photon irradiation. Since the substrate in acetonitrile shows no absorption at 775 nm, the only mechanism by which photodecomposition with the given wavelength can take place is from a two-photon initiated process.

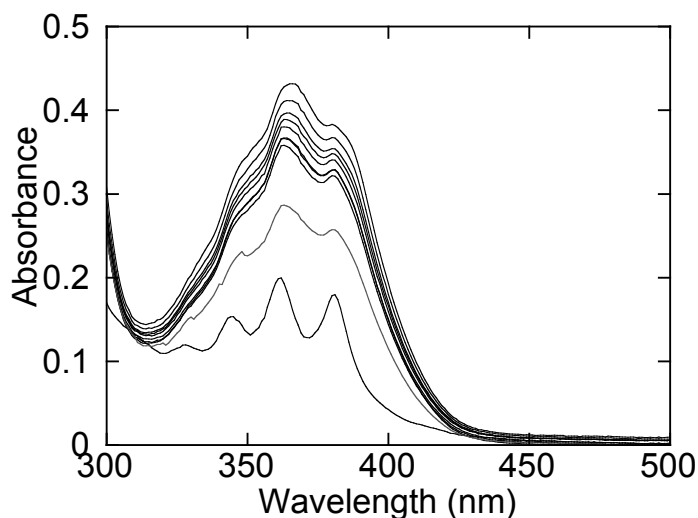


Figure 30. Absorption spectra obtained, before irradiation of a solution of *N*-anthracenoyloxypyridinethione **1g** in acetonitrile; after 775 nm femtosecond irradiation of **1g** solution at 20 min intervals (from 20 min to 160 min); after 775 nm femtosecond irradiation of **1g** solution for 360 min and after exposure of **1g** solution to room light for 5 min. Absorption spectra are presented sequentially in the order they were presented in the caption, with the absorption spectra before irradiation of **1g** solution corresponding to the highest absorbance.

To obtain the two-photon cross section using eq. 5, the absorbance measurements were used to obtain values for  $C_t/C_o$  according to eq. 5.6.

$$\frac{C_t}{C_o} = \frac{Abs_t - Abs_\infty}{Abs_o - Abs_\infty} \quad (5.6)$$

In this equation,  $Abs_t$  is the absorption at the maximum wavelength of 367 nm after each period of femtosecond irradiation,  $Abs_o$  is the absorption at 367 nm prior to irradiation, and  $Abs_\infty$  is the absorbance after complete decomposition of the substrate. This data was plotted as a function of the corrected irradiation time to give the plot shown in Figure 31. Non-linear least squares fitting of the data to eq. 5 gave a two-photon cross section  $\delta = 0.053 \text{ GM}$ .

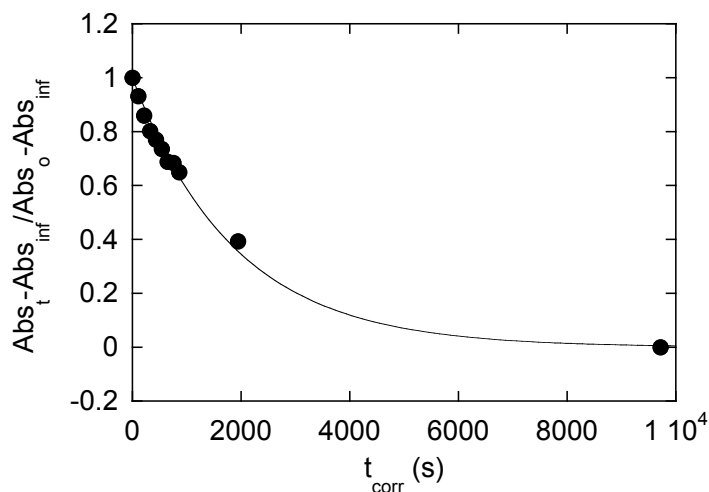


Figure 31. Relationship between absorption by a solution of *N*-anthracenoyloxypyridinethione **1g** in acetonitrile at 367 nm and corrected femtosecond irradiation time. Note that the final point is the absorbance after complete decomposition, and it was arbitrarily placed at  $10^4$  s.

The measured two-photon cross section,  $\delta = 0.053$ , for decomposition of **1g** was disappointingly small, being less than then the decomposition two-photon cross section for *N*-naphthoyloxypyridinethione **1c** ( $\delta = 0.21$ ), and not much greater than that for *N*-benzoyloxypyridinethione **1b** ( $\delta = 0.051$ ).

It is not presently known why the anthracene group did not provide the expected enhancement in the two-photon cross section. Several possibilities exist, including that our initial hypothesis that a charge-transfer relationship between the pyridinethione ring and the aryl group of the carboxylate moiety increases the probability of two-photon excitation is incorrect, and more data is clearly needed to make firm conclusions. However, one possibility that must be considered is that the anthracenyl group is absorbing the 775 nm light in addition to the pyridinethione group. It is known that anthracene is susceptible to two-photon excitation, although its two-photon cross section has not yet been measured. If so, it could be that the less than expected efficiency is simply due to a fraction of the 775 nm light that is being used to induce two-photon excitation of the anthracene group, which presumably does not lead to photodecomposition of the substrate.

Future work in this area would presumably involve using one of the other approaches outlined in the introduction, namely modifying the carboxylate group in other ways to enhance the probability of achieving the desired orientation of the two aryl groups, or by adding electron donating and/or withdrawing groups to the aryl group of the carboxylate moiety to modulate the efficiency of the proposed charge-transfer interaction.

## CHAPTER 5 EXPERIMENTAL

### 5.1 General Methods

All reactions were performed under an atmosphere of nitrogen unless stated otherwise. Glassware was oven-dried prior to use. Starting materials were used as received from commercial sources, without further purification, unless otherwise noted. Reaction progress was monitored by thin layer chromatography (TLC) using EMD Chemicals pre-coated plastic-backed silica plates (silica gel 60, F254). Visualization was accomplished with ultraviolet light. Purification of reaction products was achieved by flash chromatography using Silicycle silica gel (Silica P-Flash, 40-63  $\mu\text{m}$  particle size, 230-240 mesh) and the specified mobile phase. Solvents were removed under reduced pressure using a Brinkmann Rotovapor.

Melting points were measured on a Fisher-Johns melting point apparatus and are uncorrected.  $^1\text{H}$ , and proton-decoupled  $^{13}\text{C}$  nuclear magnetic resonance spectra (NMR) were recorded using a Bruker Avance 500 MHz spectrometer.  $^1\text{H}$  NMR spectra were recorded in  $\text{CDCl}_3$  and chemical shifts have been reported in parts per million (ppm) downfield from tetramethylsilane (TMS) as the internal standard or relative to chloroform,  $\text{CHCl}_3$  ( $\delta$  7.27). Proton-decoupled  $^{13}\text{C}$  spectra were recorded in  $\text{CDCl}_3$  with chemical shifts reported in ppm relative to solvent ( $\delta$  77.0). Mass spectra were provided by the Dalhousie University Mass Spectrometry laboratory using a Bruker Focus orthogonal ESI-microTOF mass spectrometer. Sample introduction flow rate was 2  $\mu\text{L}/\text{min}$ , capillary 4500 v, and dry gas flow rate of 4 L/min.

## 5.2 Synthesis of Compounds **1b** - **1g**

All syntheses were performed in the absence of light as to not induce any unwanted photodecomposition. Reaction vessels were covered with aluminum foil and NMR characterization was done using amber tinted NMR tubes. Known compounds with physical and/or spectral data reported are identified with a reference immediately following their name.

***N*-Benzoyloxypyridinethione **1b**.**<sup>[55]</sup> To a solution of *N*-(hydroxy)pyridine-2-thione sodium salt (2.00 g, 16.0 mmol) in dichloromethane (DCM) (32 mL), a molar equivalent of benzoyl chloride (1.83 mL, 16.0 mmol) was added drop wise over a 10 min period. A 30 % excess of pyridine (1.52 mL, 20.8 mol) was added and the reaction mixture was diluted with DCM (50 mL). The reaction mixture was then extracted in a separatory funnel with saturated aqueous sodium bicarbonate (2 X 50 mL). The organic layer was dried over anhydrous magnesium sulfate and the solvent was evaporated under reduced pressure yielding crude product. The product was purified in a flash column (3:2 ethyl ether: hexane) and recrystallized from DCM. Yield: 1.16 g (58 %). <sup>1</sup>H NMR (CDCl<sub>3</sub>): δ 6.75-6.67 (1H, dt, *J* = 1.5, 7.0 Hz), 7.27-7.18 (1H, m), 7.56-7.46 (2H, m), 7.73-7.63 (3H, m), 8.25-8.15 (2H, d, *J* = 8.0 Hz); Low-RES MS (ESI+): *m/z* 254 (M + Na)<sup>+</sup>. The NMR spectrum matched that from the literature.<sup>[55]</sup>

***N*-Naphthoyloxypyridinethione **1c**.**<sup>[37]</sup> To a solution of *N*-(hydroxy)pyridine-2-thione (2.5 g, 20.0 mmol) in DCM (20 mL), one molar equivalent of 1-naphthoyl chloride (3.8 g, 20.0 mmol) was added drop-wise over a 10 min period followed by 4-

dimethylaminopyridine (DMAP) (2.1 g, 17.1 mmol). The reaction mixture was allowed to stir at room temperature for 24 h. The solvent was removed by evaporation under reduced pressure and crude product was recrystallized from ethyl acetate: hexane solution. Yield: 1.17 g (23 %). <sup>1</sup>H NMR (500 MHz, CDCl<sub>3</sub>): δ 6.69-6.72 (1H, dt, *J* = 1.5, 6.9 Hz), 7.28 (1H, m), 7.61-7.62 (1H, t, *J* = 7.5 Hz), 7.66-7.68 (1H, t, *J* = 7.5 Hz), 7.75-7.76 (2H, t, *J* = 6 Hz), 7.92-7.94 (1H, d, *J* = 8.0 Hz), 7.97-7.99 (1H, d, *J* = 8.5 Hz), 8.02-8.03 (1H, d, *J* = 8.0 Hz), 8.17-8.19 (1H, dd, *J* = 2.0, 10.0 Hz), 8.89 (1H, s); Low-Res MS (ESI+): *m/z* 304 (M + Na)<sup>+</sup>. Confirmed with APCI MS.

***N*-Acetoxypyridinethione 1d.**<sup>[126]</sup> To a solution of *N*-(hydroxy)pyridine-2-thione (2.00 g, 16.0 mmol) in DMF (32 mL) and pyridine (1.5 mL), one molar equivalent of acetyl chloride (1.137 mL, 16.0 mmol) was added drop-wise over a 10 min period. The solution was stirred at room temperature for 1.5 h resulting in a clear yellow reaction mixture. The reaction mixture was then extracted with saturated aqueous sodium bicarbonate (2 x 25 mL) and dried over anhydrous magnesium sulfate. The solvent was removed by evaporation under reduced pressure. The resulting crude product was recrystallized from DCM. Yield: 1.35 g (67 %). <sup>1</sup>H NMR (CDCl<sub>3</sub>): δ 2.48 (3H, s), 6.60-6.63 (1H, dt, *J* = 1.5, 7.0 Hz), 7.16-7.19 (1H, dt, *J* = 1.5, 6.9 Hz), 7.54-7.56 (1H, dd, *J* = 1.0, 7.0 Hz), 7.66-7.68 (1H, dd, *J* = 1.5, 8.8 Hz). The NMR spectrum matched that from the literature.<sup>[126]</sup>

***N*-Benzyloxypyridinethione 1e.**<sup>[127]</sup> Benzyl mesylate was prepared according to procedure of Crossland and Servis.<sup>[128]</sup> To a 0.2 M solution of benzyl alcohol (0.585 mL, 5 mmol) in methylene chloride was added a 50 % molar excess of triethylamine (0.585



mL, 10 mmol) at 0 °C, followed by a 10 % excess of methanesulfonyl chloride (0.430 mL, 5.5 mmol) added drop-wise over a period of 10 min. The resulting solution was stirred for an additional 15 min keeping the temperature at 0 °C. The next steps were done keeping using pre-chilled glassware. The reaction mixture was transferred to a separatory funnel with the aid of additional methylene chloride. The reaction mixture was first extracted with ice water (2 X 10 mL), followed by cold 10 % hydrochloric acid (2 X 10 mL), saturated sodium bicarbonate solution (2 X 10 mL), and brine (2 X 10 mL). Drying of the solution with anhydrous magnesium sulfate followed by the evaporation of solvent under reduced pressure yielded benzyl mesylate (0.92 g, 5.1 mmol). The resulting mesylate was combined in a 1:1 molar ratio with *N*-(hydroxy)pyridine-2-thione sodium salt (0.762 g, 5.1 mmol) in DMF (19 mL) and stirred at 0°C for 1 h. The DMF was removed from the resulting yellow solution by evaporation under reduced pressure and the residue was taken up in 0.1 M NaOH (10 mL) and ether (15 mL). Insoluble matter was removed *via* filtration and the two-phase mixture was transferred to a separatory funnel. The aqueous phase was extracted with ether (10 mL portions) until no yellow color was observed in the organic layer. The combined ether extracts were washed with saturated aqueous sodium bicarbonate (2 X 10 mL) and then with brine (2 X 10 mL). Drying of the solution over anhydrous magnesium sulfate followed by the evaporation of the solvent under reduced pressure gave the crude product as yellow/brown oil. This was purified using flash column chromatography (ether) to yield pure product as yellow/brown crystals, after evaporation of solvent under reduced pressure. Yield: 0.191 g (21%). mp: 72-75 °C (Lit<sup>[126]</sup> mp: 74-77 °C); <sup>1</sup>H NMR (CDCl<sub>3</sub>): δ 5.46 (2H, s), 6.39-6.41 (1H, dt, *J* = 2.0, 7.0 Hz), 7.08-7.11 (1H, dt, *J* = 1.5, 6.9 Hz), 7.23-7.48 (6H, m), 7.65

(1H, dd,  $J = 1.0, 7.0$  Hz); Low-Res MS (ESI+):  $m/z$  240 (M + Na)<sup>+</sup>. The NMR spectrum matched that from the literature.<sup>[126]</sup>

***N-t-Butoxypyridinethione 1f.***<sup>[126]</sup> The reaction of *N*-(hydroxy)pyridine-2-thione sodium salt (1.64 g, 11.0 mmol) with *t*-butyl bromide (1.51 g, 11.0 mmol) in DMF (50 mL) stirring at 40 °C for 15 h resulted in a slightly yellow solution. The solvent was evaporated under reduced pressure and the resulting residue was taken up in 0.1 M aqueous NaOH (15 mL) and ether (22 mL). The two-phase mixture was transferred to a separatory funnel and the aqueous layer was extracted with ether (10 mL portions) until no yellow color remained in the organic layer. Combined ether extracts were washed with saturated aqueous sodium bicarbonate (2 X 10 mL) and then with brine (2 X 10 mL). The solution was dried over anhydrous magnesium sulfate followed by the evaporation of the solvent under reduced pressure to yield product. Yield: 3.75 mg (0.2 %). <sup>1</sup>H NMR (CDCl<sub>3</sub>): δ 1.54 (9H, s), 6.56-6.67 (1H, dt,  $J = 1.5, 6.9$  Hz), 7.09-7.12 (1H, dt,  $J = 2.0, 7.0$  Hz) 7.63-7.71 (2H, m); Low-Res MS (ESI+):  $m/z$  206 (M + Na)<sup>+</sup>.

***N-Anthracenoyloxypyridinethione 1g.*** 9-Anthracenecarboxylic acid (0.69 g, 3.11 mmol) and *N*-(hydroxy)pyridine-2-thione (4.13 g, 3.73 mmol) were combined with *N,N'*-dicyclohexylcarbodiimide (DCC) (1.28 g, 6.2 mmol) in the presence of DMAP (38 mg, 0.31 mmol) in DCM (30 mL). Solvent was removed under reduced pressure yielding a yellow solid. The yellow solid was purified in a flash column (ethyl acetate/hexane (1:5)). Fractions 3-12 were collected and the solvent was removed under reduced pressure. The resulting material was recrystallized from ethanol. Yield: 0.35 g (36 %).

Mp: 177-180 °C.  $^1\text{H}$  NMR ( $\text{CDCl}_3$ ):  $\delta$  6.75-6.77 (1H, dt,  $J = 1.0, 6.5$  Hz), 7.27-7.31 (1H, t,  $J = 8.0$  Hz), 7.54-7.57 (2H, t,  $J = 7$  Hz), 7.65-7.68 (2H, t,  $J = 8.0$  Hz), 7.84-7.85 (2H, d,  $J = 7.5$  Hz), 8.06-8.08 (2H, d,  $J = 8.5$  Hz), 8.68 (1H, s), 8.73-8.75 (2H, d,  $J = 9$  Hz);  $^{13}\text{C}$  proton-decoupled NMR ( $\text{CDCl}_3$ ):  $\delta$  113.0, 125.4, 125.9, 128.1, 125.9, 130.1, 133.5, 137.7, 138.2, carbonyl and thione carbons could not be detected. High-Res MS (ESI+):  $m/z$  calcd for  $\text{C}_{20}\text{H}_{13}\text{NNaOS}$ : 354.0559, found: 354.0565.

### 5.3 Materials and Methods of DNA Studies

Supercoiled pBR 322 plasmid DNA (form I, MW  $2.9 \times 10^6$  D, 4365 bp) buffered in solution (10 mM Tris-HCl, pH 8.0, 1 mM EDTA) was purchased from Sigma Aldrich and Thermo Scientific. Ethidium bromide (10 mg/mL), bromophenol blue gel-loading solution, agarose powder, and 50X TAE premixed nucleic acid electrophoresis buffer (tris, acetic acid, EDTA, pH 8.0) were all purchased from Biorad and used as received. Gel electrophoresis was done in a Biorad mini-sub cell system, which was equipped with a Biorad basic Powerpac as a power supply. DNA spots were detected by exposure to a DNR MF-ChemBis 3.2 Bio-Imaging system UV transilluminator (254 nm) and recorded using GelCapture software. The ratio of open-circular DNA relative to the total amount was determined from the light intensity of the bands using GelEval software. Sample irradiation was done with a Clark-MXR CPA-2001 titanium:sapphire femtosecond laser (775 nm, 1000 Hz,  $\leq 600$   $\mu\text{J}/\text{pulse}$ ,  $\leq 0.20$  ps/pulse).

### *5.3.1 Laser Irradiation Experiments: Modification of pBR 322 DNA*

The reactions were carried out in Eppendorf tubes with buffered supercoiled pBR 322 DNA (0.5  $\mu\text{g}/\mu\text{L}$ ). Samples of 10.0  $\mu\text{L}$  final volume were prepared from stock pBR 322 DNA (5.0  $\mu\text{l}$ ) and **1a - f** (4.45 mM in acetonitrile, 5.0  $\mu\text{L}$ ). The resulting solutions were irradiated with the Clark-MXR CPA-2001 femtosecond laser (775 nm, 1000 Hz,  $\leq 600 \mu\text{J}/\text{pulse}$ ,  $\leq 0.20 \text{ ps}/\text{pulse}$ ) for 3 h from above at a distance of approximately 20 cm in an open Eppendorf tube wrapped with transparent DuraSeal plastic to prevent loss of sample through evaporation.

### *5.3.2 Determination of Strand Breaks by Gel Electrophoresis*

Following irradiation, 2.0  $\mu\text{L}$  of bromophenol blue 6X dye (0.25 % bromophenol blue (W/V), 40 % sucrose (W/V), in distilled water) was added to the samples in the Eppendorf tubes. Agarose gel (1 %) was prepared by microwave heating of agarose (0.4 g) and 1X TAE buffer (40 mL) in a high-power microwave oven (600 W) with stirring every 20 s until all agarose was completely dissolved. The agarose solution was allowed to cool to  $\sim 60^\circ\text{C}$  and ethidium bromide (2  $\mu\text{L}$ ) was added. The solution was then poured into the mold casing, the comb was inserted, and it was allowed to cool for 45 min, upon cooling and solidification of the matrix gel, the comb was carefully removed leaving 8 wells in the gel. The gel was then inserted into the electrophoresis apparatus, and it was filled with 1X TAE buffer to a height of approximately 1 mm above the gel surface. 10.0  $\mu\text{L}$  aliquots of irradiated samples and 6X loading dye were transferred into the gel wells using a pipette. Electrophoresis was then carried out at 45 V for 3 h. The resulting gels

were photographed under exposure to a UV transilluminator and analyzed using GelEval software.

#### *5.4 Procedure for Measuring Two-photon Cross Section*

A solution of *N*-anthracenoyloxypyridinethione **1g** in acetonitrile was prepared in a cuvette so that the absorption at 367 nm was about 0.4. The cuvette used in this work was 3 mm x 10 mm cuvette with space at the bottom of the cuvette for a small stirring bar. The total volume of the solution was 1.5 mL. During preparation and handling, the cuvette with the solution was kept in the dark.

After measuring the absorption spectrum prior to irradiation (using a Cary 100 UV-Vis spectrophotometer), the cuvette was placed in a sample holder above a stir plate, and the cuvette exposed to the Clark-MXR CPA-2001 femtosecond laser (775 nm, 1000 Hz,  $\leq 600 \mu\text{J}/\text{pulse}$ ,  $\leq 0.20 \text{ ps}/\text{pulse}$ ) for the desired time. The solution was stirred throughout. The cuvette was then removed and an absorption spectrum obtained. This procedure was repeated until the sample showed at least 50 % photodecomposition. The solution was then exposed to room light for 5 min to obtain the infinity absorption reading.

## CHAPTER 6 CONCLUSIONS AND FUTURE WORK

### *6.1 Conclusions and Future Work: DNA Strand Cleavage Study*

The study of *N*-alkoxy pyridinethiones showed the utility of two-photon excitation in the biological application of DNA cleavage, specifically that alkoxy radicals generated upon pulsed femtosecond laser irradiation, 775 nm, are able to induce a significant quantity of single strand breaks in cell-free duplex pBR 322 DNA. The efficiency of the alkoxy radicals, to induce strand cleavage, was found to vary depending on its substituent group. This variance is thought to be attributed to several factors, most notably: radical stability, the two-photon cross section of the substrate, and the substrate's ability to intercalate with the DNA duplex prior to radical formation. The parent compound *N*-hydroxy pyridinethione **1a** was found to be the most efficient DNA strand cleaver. This is most likely attributed to the extreme reactivity of  $\cdot\text{OH}$  radicals with duplex DNA. As mentioned earlier the issue of non-specificity can arise when looking forward with **1a**, particularly when this compound is introduced into a whole-cell environment. **1a** efficiency has been found to wane in such cases in one-photon excitation studies, and under the assumption that a radical generated through a two-photon process will behave in the same manner as that generated in a one-photon process, despite displaying the highest efficiency in these experiments **1a** may not be the compound of choice when moving forward. Alkoxy derivatives of **1a**, compounds **1b - f**, though found to be less efficient strand cleavers, provide a specific source of radical generation. This is a significant quality, as when moving into whole-cell studies compounds **1b - f** will lack the aqueous equilibrium that **1a** exists in. This will allow compounds **1b - f** to more efficiently produce a larger quantity of the desired radicals, in biological media. In saying

this, it is suggested that future work in cell-free environments explores such alkoxy derivatives, using trends and observations made in this study to allow for a reference point when considering more complex substituent groups. Enhancing the two-photon cross section of these compounds should be viewed with utmost importance, continuing work analogous to that done in the second project. As well, enhancement of DNA intercalating properties should be explored, as this was found to potentially have a significant role in cleaving efficiency in this study.

### *6.2 Conclusions and Future Work: Photodecomposition Study*

The goal of this study was achieved in measuring a two-photon cross section for decomposition of *N*-anthracenoyloxypyridinethione **1g**. This value,  $\delta = 0.053$  GM, was found to be disappointingly small when compared to the hypothesized cross section, which was expected to be greater than that of *N*-naphthoyloxypyridinethione **1c**,  $\delta = 0.21$  GM. This lower value brings the previously suggested theory of charge-transfer relation between the aryl group and the pyridinethione ring into question, yet as mentioned earlier this could be due to the anthracene group absorbing simultaneously at 775 nm. There are several possibilities that arise for the future direction of this work, including observing the effect of electron donating/withdrawing substituent groups on the aryl moiety, and increasing the alkane chain length between the radical center and the aryl group making a charge-transfer conformation more accessible.

Future work in this project works alongside with that of the first project. Optimization of two-photon cross section will allow for potentially more effective DNA cleaving compounds, due to more efficient radical generation. An effort should be put be

forward to streamline these two projects in the future, looking first at maximizing the two-photon cross section value of a compound before employing it in biological studies. This suggestion is strongly supported by *N*-naphthoyloxy pyridinethione **1c** having the highest reported two-photon cross section value,  $\delta = 0.21$  GM, and being the most efficient DNA cleaver in terms of *N*-alkoxy pyridinethiones investigated in this work.



## REFERENCES

- [1] Goeppert-Mayer, M., *Ann. Phys.* **1931**, *401*, 273-294.
- [2] Maiman, T. H., *Nature*. **1960**, *187*, 493-494.
- [3] Kaiser, W.; Garrett, C. G. B., *Phys. Rev. Lett.* **1961**, *7*, 229-231.
- [4] Peticolas, W. L.; Goldsborough, J. P.; Rieckhoff, K. E., *Phys. Rev. Lett.* **1963**, *10*, 43-45.
- [5] Peticolas, W. L.; Rieckhoff, K. E. J., *Chem. Phys.* **1963**, *39*, 1347-1348.
- [6] Pawlicki, M.; Collins, H. A.; Denning, R. G.; Anderson, H. L., *Angew. Chem. Int. Ed.* **2009**, *48*, 3244-3266.
- [7] Parthenopoulos, A. D.; Rentzepis, M. P., *Science*. **1989**, *245*, 843-845.
- [8] Denk, W.; Strickler, J. H.; Webb, W. W., *Science*. **1990**, *248*, 73-76.
- [9] Kawata, S.; Kawata, Y., *Chem. Rev.* **2000**, *100*, 1777-1788.
- [10] Spangler, C. W., *J. Mater. Chem.* **1999**, *9*, 2013-2020.
- [11] LaFratta, C. N.; Fourkas, J. T.; Baldacchini, T.; Farrer, R. A., *Angew. Chem. Int. Ed.* **2007**, *46*, 6238-6258.
- [12] Lin, T. C.; Chung, K. S.; Kim, K. S.; Wang, X.; He, G. S.; Swiatkiewicz, H. E.; Pudavar, H. E.; Prasad, P. N., *Adv. Polym. Sci.* **2003**, *161*, 157-193.
- [13] Calvete, M.; Yang, G. Y.; Hanack, M., *Synth. Met.* **2004**, *141*, 231-243.
- [14] Strehmel, B.; Strehmel, V., *Adv. Photochem.* **2007**, *29*, 111-354.
- [15] Rumi, M.; Barlow, S.; Wang, J.; Perry, J. W.; Marder S. R., *Adv. Polym. Sci.* **2008**, *213*, 1-95.
- [16] He, G. S.; Tan, L. S.; Zheng, Q.; Prasad, P. N., *Chem. Rev.* **2008**, *108*, 1245-1330.

- [17] Terenziani, F.; Katan, C.; Badaeva, E.; Tretiak, S.; Blanchard-Desce, M., *Adv. Mater.* **2008**, *20*, 4641-4678.
- [18] Kim, H. M.; Cho, B. R., *Chem. Commun.* **2009**, 153-164.
- [19] Fisher, W. G.; Partridge Jr.; W. P.; Dees, C.; Wachter, E. A., *Photochem. Photobiol.* **1997**, *66*, 141-155.
- [20] Ellis-Davies, G. C. R., *Nat. Methods.* **2007**, *4*, 619-628.
- [21] Belfield K. D.; Bondara M. V.; Przhonska O. V., *J. Fluoresc.* **2006**, *16*, 111-117.
- [22] Marder, S. R.; Bredas, J.; Perry, J. W., *MRS Bulletin.* **2007**, *32*, 561-565.
- [23] Stamatis, C., *INTERSUN: The Global UV Project.* World Health Organization. **2003**.
- [24] Pawlicki, M.; Collins, H. A.; Denning, R. G.; Anderson, H. L., *Angew. Chem. Int. Ed.*, **2009**, *48*, 3244-3266.
- [25] Ventelon, L.; Charier, S.; Moreaux, L.; Mertz, J.; Blanchard-Desce, M., *Angew. Chem.* **2001**, *40*, 2098-2101.
- [26] Xu, C.; Webb, W. W., *J. Opt. Soc. Am. B.* **1996**, *13*, 481-491.
- [27] Karotki, A.; Drobizhev, M.; Kruk, M.; Spangler, C.; Nickel, E.; Mamardashvili, N.; Rebane, A. *J. Opt. Soc. Am. B* **2003**, *20*, 321-332..
- [28] Makarov, N. S.; Drobizhev, M.; Rebane, A., *Opt. Express.* **2008**, *16*, 4029-4047.
- [29] Gould. R. G., In Franken, P.A. and Sands, R.H. (Eds.). *The Ann Arbor Conference on Optical Pumping*, University of Michigan. **1959**, 128.
- [30] Riley, P. A., *Int. J. Rad. Biol.* **1994**, *65*, 27-33.
- [31] Walling, C., *Acc. Chem. Res.* **1975**, *8*, 125-132.

- [32] Von Sonntag, C., *The chemical basis of radiation biology*. London: Taylor and Francis; **1987**.
- [33] Boivin, J.; Crepon, E.; Zard, S. Z., *Tetrahedron Lett.* **1990**, *31*, 6869-6872.
- [34] Adam, W.; Ballmaier, D.; Epe, B.; Grimm, G. N.; Saha-Moller, C. R., *Angew. Chem. Int. Ed. Engl.* **1995**, *34*, 2156–2158.
- [35] Epe, B.; Ballmaier, D.; Adam, W.; Grimm, G. N.; Saha-Moller, C. R., *Nucleic Acid Res.* **1996**, *24*, 1625-1631.
- [36] Adam, W.; Hartung, J.; Okamoto, H.; Saha-Moller, C. R.; Spehar, K., *Photochem. Photobiol.* **2000**, *72*, 619-624.
- [37] Theodorakis, E. A.; Wilcoxon, K. M., *Chem. Commun.* **1996**, 1927-1928.
- [38] Adam, W.; Marquardt, S.; Saha-Moller, C. R., *Photochem. Photobiol.* **1999**, *70*, 287-291.
- [39] Aveline, B. M.; Kochevar, I. E.; Redmond, R. W., *J. Am. Chem. Soc.* **1996**, *118*, 10124-10133.
- [40] Adam, W.; Grimm, G. N.; Saha-Moller, C. R., *Free Radical Biol. Med.* **1998**, *24*, 234-238.
- [41] Dizdaroglu, M.; Jaruga, P., *Free Radical Res.* **2012**, *46*, 382-419.
- [42] Sies, H., ed. *Oxidative stress, oxidants and antioxidants*. New York: Academic Press; **1991**.
- [43] Breen, A. P.; Murphy, J. A., *Free Radical Biol. Med.* **1995**, *18*, 1033-1077.
- [44] Blake, D. R.; Allen, R. E.; Lunec, J., *Br. Med. Bull.* **1987**, *43*, 371-385.
- [45] Harman, D., *J. Gerontol.* **1985**, *11*, 298-300.
- [46] Sohal, R. S., *Adv. Myochem.* **1989**, *2*, 21-34.

- [47] Sohal, R. S., *Aging Milano*. **1993**, 5, 3-17.
- [48] Halliwell, B.; Gutteridge, J. M. C., *Free radicals in biology and medicine*. Oxford: Oxford University Press; **1989**.
- [49] Legrand-Poels, S.; Hoebeke, M.; Vaira, D.; Rentier, B.; Piette, J., *J. Photochem. Photobiol. B: Biol.* **1993**, 17, 229-237.
- [50] Aust, A. E.; Eveleigh, J. F., *Proceedings of the society for experimental biology and medicine*. **1999**, 222, 246-252.
- [51] Dizdaroglu, M.; Jaruga, P.; Birinioglu, M.; Rodriguez, H., *Free Radical Biol. Med.* **2002**, 32, 1102-1115.
- [52] Theodorakis, E. A.; Xiang, X.; Lee, M.; Gibson, T., *Tetrahedron Lett.* **1998**, 39, 3383-3386.
- [53] Von Sonntag C. *Free-radical-induced DNA damage and its repair*. Hiedelberg: Springer; **2006**.
- [54] Pratviel, G.; Bernadou, J.; Meunier, B., *Angew. Chem., Int. Ed. Engl.* **1995**, 34, 746-769.
- [55] Blom, P.; Xiang, A. X.; Kao, D.; Theodorakis, E. A., *Bioorgan. Med. Chem.* **1999**, 7, 727-736.
- [56] Sigman, D. S.; Chen, C.-H., *Annu. Rev. Biochem.* **1990**, 59, 207-236.
- [57] Dervan, P. B., *Nature*. **1992**, 359, 87-88.
- [58] Huber, P. W., *Genes Dev.* **1993**, 7, 1367-1376.
- [59] Kane, S. A.; Hecht, S. M., *Prog. Nucleic Acid Res. Mol. Biol.* **1994**, 49, 313-352.
- [60] Henderson, D.; Hurley, L. H., *Nature Med.* **1995**, 1, 525-527.
- [61] Danishefsky, S. J.; Shair, M. D., *J. Org. Chem.* **1996**, 61, 16-44.

- [62] Nicolaou, K. C.; Pitsinos, E. N.; Theodorakis, E. A.; Saimoto, H.; Wrasidlo, W., *Chem. Biol.* **1994**, *1*, 57-66.
- [63] Guyton, K. Z.; Kensler, T. W., *Br. Med. Bull.* **1993**, *49*, 523-544.
- [64] Khan, A. U.; Wilson, T., *Chem. Biol.* **1995**, *2*, 437-445.
- [65] D'Aurora, V.; Stern, A. M.; Sigman, D. S., *Biochem. Biophys. Res. Commun.* **1978**, *80*, 1025-1032.
- [66] Hertzberg, R. P.; Dervan, P. B., *J. Am. Chem. Soc.* **1982**, *104*, 313-315.
- [67] Dixon W. J.; Hayes, J. J.; Levin, J. R.; Weidner, M. F.; Dombroski, B. A.; Tullius, T. D., *Methods Enzymol.* **1991**, *208*, 380-413.
- [68] Kane, S. A.; Sasaki, H.; Hecht, S. M., *J. Am. Chem. Soc.* **1995**, *117*, 9107-9118.
- [69] Chen, X.; Woodson, S. A.; Burrows, C. J.; Rokita, S. E., *Biochemistry.* **1993**, *32*, 7610-7616.
- [70] Uchida, K.; Pyle, A. M.; Morii, T.; Barton, J. K., *Nucleic Acids Res.* **1989**, *17*, 10259-10279.
- [71] Nielsen, P. E., *Nucleic Acids Res.* **1992**, *20*, 2735-2739.
- [72] Becker, M. M.; Wang, J. C., *Nature.* **1984**, *309*, 682-687.
- [73] Singh, U. S.; Scannell, R. T.; An, H.; Carter, B. J.; Hecht, S. M., *J. Am. Chem. Soc.* **1995**, *117*, 12691-12699.
- [74] Wei, L. ; Shao, Y. ; Zhou, M.; Hua, H.W.; Lu, G.Y. *Org. Biomol. Chem.* **2012**, *10*, 8484-8492.
- [75] Adam, W.; Cadet, J.; Dall'Acqua, F.; Epe, B.; Ramaiah, D.; Saha-Moller, C. R., *Angew. Chem., Int. Ed. Engl.* **1995**, *34*, 107-110.

- [76] Schepp, N. P.; Green, C. J. M.; Cozens, F. L., *Photochem. Photobiol. Sci.* **2010**, *9*, 110-113.
- [77] Schepp, N., *Two-photon cross sections*. Unpublished raw data. **2009**.
- [78] Boivin, J.; Crepon, E.; Zard, S. Z., *Tetrahedron Lett.* **1990**, *31*, 6869-6872.
- [79] Barton, D. H. R.; Jaszberenyi, J. C.; Morrell, A. I., *Tetrahedron Lett.* **1991**, *32*, 311-314.
- [80] Hess, K. M.; Dix, T. A., *Anal. Biochem.* **1992**, *206*, 309-314.
- [81] Kontoghioghes, G. J.; Piga, A.; Hoffbrand, A. W., *Hematolog. Oncol.* **1986**, *4*, 195-204.
- [82] Blatt, J.; Taylor, S. R.; Kontoghiorghes, G. J., *Cancer Res.* **1989**, *49*, 2925-2927.
- [83] Shaw, E.; Bernstein, J.; Losee, K.; Lott, W. A., *J. Am. Chem. Soc.* **1950**, *72*, 4362-4384.
- [84] Van Abbe, N. J.; Baxter, P. M.; Jackson, J. J.; Bell, M. A.; Dixon, H., *Int. J. Cosmetic Sci.* **1981**, *3*, 233-240.
- [85] Crich, D.; Quintero, L., *Chem. Rev.* **1989**, *89*, 1413-1432.
- [86] Newcomb, M.; Park, S. U., *J. Am. Chem. Soc.* **1986**, *108*, 4132-4134.
- [87] Luszytk, J.; Maillard, B.; Deycard, S.; Lindsay, D. A.; Ingold, K. U., *J. Org. Chem.* **1987**, *52*, 3509-3514.
- [88] Newcomb, M.; Horner, J. H.; Filikowsli, M. A.; Ha, C.; Park, S.- U., *J. Am. Chem. Soc.* **1995**, *117*, 3674-3684.
- [89] Evans, P. G. E.; Sugden, J. K.; Van Abbe', N., *J. Pharm. Acta. Helv.* **1975**, *50*, 94-99.
- [90] Neihof, R. A.; Bailey, C. A.; Patouillet, C.; Hannan, P. J., *Arch. Environm. Contam.*

*Toxicol.* **1979**, *8*, 355-368.

[91] Reszka, K.; Chignell, C. F., *Photochem. Photobiol.* **1995**, *61*, 269-275.

[92] Boivin, J.; Crepon, E.; Zard, S. Z., *Bull. Soc. Chim. Fr.* **1992**, *129*, 145-150.

[93] Chan, H. W. -S., *Autoxidation of unsaturated lipids*. London: Academic Press; **1987**.

[94] Tallman, K. A.; Tronche, C.; Yoo, D. J.; Greenberg, M. M., *J. Am. Chem. Soc.* **1998**, *120*, 4903-4909.

[95] Rodriguez, H.; Valentine, M. R.; Holmquist, G. P.; Akman, S. A.; Termini, J., *Biochemistry.* **1999**, *38*, 16578-16588.

[96] Adam, W.; Kurz, A.; Saha-Moller, C. R., *Chem. Res. Toxicol.* **2000**, *13*, 1199-1207.

[97] Sanchez, C.; Shane, R. A.; Thomas, P.; Ingold, K. U., *Chem. Res. Toxicol.* **2003**, *16*, 1118-1123.

[98] Adam, W.; Arnold, M. A.; Grimm, G. N.; Saha-Moller, C. R.; Dall'Acqua, F.; Miolo, G.; Vedaldi, D., *Photochem. Photobiol.* **1998**, *68*, 511-518.

[99] Mahler, H.-C.; Schulz, I.; Adam, W.; Grimm, G. N.; Saha-Moller, C. R.; Epe, B., *Mutat. Res.- DNA repair.* **2001**, *461*, 289-299.

[100] Theodorakis, E.; Xiang, X.; Blom, P., *Chem. Commun.* **1997**, *15*, 1463-1464.

[101] Moan, J.; Peng, Q., *Anticancer Res.* **2003**, *23*, 3591-3600.

[102] Phillips, D., *Photochem. Photobio. Sci.* **2010**, *9*, 1589-1596.

[103] Lou, P. J.; Jones, L.; Hopper, C., *Technol. Cancer Res. Treat.* **2003**, *2*, 311-317.

[104] Hamblin, M. R.; Hassan, T., *Photochem. Photobio. Sci.* **2004**, *3*, 436-450.

[105] Bressler, N. M.; Bressler, S. B., *Invest. Ophthalmol. Vis. Sci.* **2000**, *41*, 624-628.

[106] Skovsen, E.; Synder, J. W.; Lambert, J. D. C.; Ogilby, P. R., *J. Phys. Chem. B.* **2005**, *109*, 8570-8573.

- [107] Roots, R.; Okada, S., *Radiat. Res.* **1975**, *64*, 306-320.
- [108] Egorov, S. Y.; Kamalov, V. F.; Koroteev, N. I.; Krasnovsky, A. A.; Toleutaev B. N.; Zinukov, S. V., *Chem. Phys. Lett.* **1989**, *163*, 421-424.
- [109] Skovsen, E.; Snyder, J. W.; Lambert, J. C. D.; Ogilby, P. R., *J. Phys. Chem. B.* **2005**, *109*, 8570-8573.
- [110] Kuimova, M. K.; Yahiolu, G.; Ogilby, P. R., *J. Am. Chem. Soc.* **2009**, *131*, 332-340.
- [111] Hatz, S.; Poulsen, L.; Ogilby, P. R., *Photochem. Photobiol.* **2008**, *84*, 1284-1290.
- [112] Moan, J.; Berg, K., *Photochem. Photobiol.* **1991**, *53*, 549-553.
- [113] Goyan, R. L.; Cramb, D. T., *Photochem. Photobiol.* **2000**, *72*, 821-827.
- [114] Samkoe, K. S.; Fecica, M. S.; Goyan, R. L.; Buchholz, J. L.; Campbell, C.; Kelly, N. M.; Cramb, D. T., *Photochem. Photobiol.* **2006**, *82*, 152-157.
- [115] Collins, H. A.; Mamta Khurana, M.; Moriyama, E. H.; Mariampillai, A.; Dahlstedt, E.; Balaz, M.; Kuimova, M. K.; Drobizhev, M.; Yang, V. X. D.; Phillips, D.; Rebane, A.; Wilson, B. C.; Anderson, H. L. *Nature Photonics.* **2008**, *2*, 420-424.
- [116] Svaasand, L. O.; Tromberg, B. J.; Wyss, P.; Wyss-Desserich, M. T.; Tadir, T.; Berns, M. W., *Lasers Med. Sci.* **1996**, *11*, 261-265.
- [117] Chrumbach A.; Rodbard D., *Science.* **1971**, *172*, 440-451.
- [118] Aveline, B. M.; Redmond, R. W., *Photochem. Photobiol.* **1998**, *68*, 266-275.
- [119] Adam. W.; Grimm, G. N.; Marquardt, S.; Saha-Moller, C. R., *J. Am. Chem. Soc.* **1999**, *121*, 1179-1185.
- [120] Jones, R. A.; Katritzky, A. R. J., *J. Chem. Soc.* **1960**, 2937-2942.
- [121] Chateaufneuf, J.; Luszyk, J.; Ingold, K. U., *J. Am. Chem. Soc.* **1988**, *110*, 2886-2893.



- [122] Richards, A. D.; Rodgers, A., *Chem. Soc. Rev.* **2007**, *36*, 471-483.
- [123] Salganik, R. I.; Dianov, G. L., *Mutat. Res.* **1992**, *266*, 163-170.
- [124] Halverson-Smith, D., *Dalhousie University Honours Project.* **2011**.
- [125] Poloukhine, A.; Popik, V. V.; Uradabayev, N. K., *Chem. Commun.* **2006**, *4*, 454-456.
- [126] Barton, D. H. R.; Tachdjian, C., *Tetrahedron.* **1992**, *48*, 7109-7120.
- [127] Hay, B. P.; Beckwith, A. L. J., *J. Org. Chem.* **1989**, *54*, 4330-4334.
- [128] Crossland, R. K.; Servis, K. L., *J. Org. Chem.* **1970**, *35*, 3195-3196.

## APPENDIX COPYRIGHT PERMISSION

Rightslink Printable License

2013-08-16 2:35 PM

### CAMBRIDGE UNIVERSITY PRESS LICENSE TERMS AND CONDITIONS

Aug 16, 2013

---

This is a License Agreement between Michael Ruzik-Gauthier ("You") and Cambridge University Press ("Cambridge University Press") provided by Copyright Clearance Center ("CCC"). The license consists of your order details, the terms and conditions provided by Cambridge University Press, and the payment terms and conditions.

**All payments must be made in full to CCC. For payment instructions, please see information listed at the bottom of this form.**

License Number	3210290341788
License date	Aug 15, 2013
Licensed content publisher	Cambridge University Press
Licensed content publication	MRS Bulletin
Licensed content title	Materials for Multiphoton 3D Microfabrication
Licensed content author	Seth R. Marder, Jean-Luc Brédas and Joseph W. Perry
Licensed content date	Jul 1, 2007
Volume number	32
Issue number	07
Start page	561
End page	565
Type of Use	Dissertation/Thesis
Requestor type	Author
Portion	Text extract
Number of pages requested	1
Author of this Cambridge University Press article	No
Author / editor of the new work	Yes
Order reference number	
Territory for reuse	World
Title of your thesis / dissertation	CLEAVAGE OF DUPLEX DNA USING TWO-PHOTON EXCITATION OF N-(ALKOXY)PYRIDINE THIONES
Expected completion date	Aug 2013
Estimated size(pages)	110
Billing Type	Invoice

<https://s100.copyright.com/CustomAdmin/PLF.jsp?ref=45d7cc17-e074-4e27-ad76-27b7503b660c>

Page 1 of 2

**Billing address** Department of Chemistry  
Dalhousie University  
Halifax, NS B3H4R2  
Canada

**Total** 0.00 USD

**Terms and Conditions**

Terms and Conditions are not available at this time.

**If you would like to pay for this license now, please remit this license along with your payment made payable to "COPYRIGHT CLEARANCE CENTER" otherwise you will be invoiced within 48 hours of the license date. Payment should be in the form of a check or money order referencing your account number and this invoice number RLNK501091225.**

**Once you receive your invoice for this order, you may pay your invoice by credit card. Please follow instructions provided at that time.**

**Make Payment To:  
Copyright Clearance Center  
Dept 001  
P.O. Box 843006  
Boston, MA 02284-3006**

**For suggestions or comments regarding this order, contact RightsLink Customer Support: [customercare@copyright.com](mailto:customercare@copyright.com) or +1-877-622-5543 (toll free in the US) or +1-978-646-2777.**

**Gratis licenses (referencing \$0 in the Total field) are free. Please retain this printable license for your reference. No payment is required.**

---